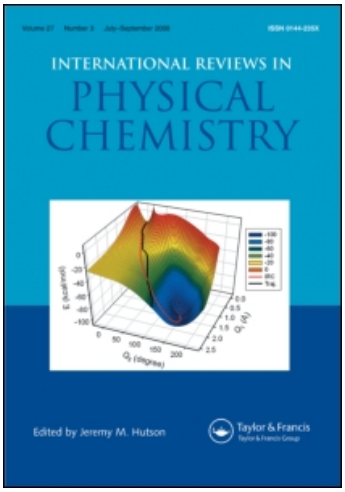

International Reviews in Physical Chemistry
Publication details, including instructions for authors and subscription information:
http://www.informaworld.com/smpp/title~content=t713724383

Solution chemistry in silicon

G. F. Cerofolini[ab]; L. Meda[a]
[a] SGS-Thomson Microelectronics, Agrate Mi, Italy [b] EniChem, Milano, Mi, Italy

To cite this Article Cerofolini, G. F. and Meda, L.(1988) 'Solution chemistry in silicon', International Reviews in Physical Chemistry, 7: 2, 123 — 171
To link to this Article: DOI: 10.1080/01442358809353209
URL: http://dx.doi.org/10.1080/01442358809353209

INTERNATIONAL REVIEWS IN PHYSICAL CHEMISTRY, 1988, VOL. 7, NO. 2, 123–171

Solution chemistry in silicon

by G. F. CEROFOLINI† and L. MEDA
SGS-Thomson Microelectronics, 20041 Agrate MI, Italy

For about the past two centuries, the chemistry of solutions has been the chemistry of aqueous solutions. Only in recent years have different environments, ammonia in particular, been extensively studied. In the last forty years, however, the industrial relevance of germanium and silicon electronic devices has provoked interest in solid solutions of almost all elements in these semiconductors. In this article, concepts taken from the physics of semiconductors and the chemistry of solutions will be brought together in an attempt at founding a new chapter of physical chemistry—solution chemistry in silicon.

There are seven sections as follows. Section 1 considers the various phases of silicon which can be obtained from diamond-cubic silicon. One kind of amorphous silicon, obtained by ion implantation, in particular, is discussed. Section 2 is devoted to equilibrium defects in silicon which remain in the thermodynamic limit—vacancies, self-interstitials and Frenkel pairs. The role of surfaces is emphasized. Section 3 considers the major impurities as they are found in a silicon ingot because of the growth technique and evolution during subsequent heat treatments. Section 4 describes the most important (both from the conceptual and technological points of view) impurities in silicon, i.e. Group III acceptors and Group V donors. The limits of applicability of the effective-mass approximation to the calculation of the electronic properties of these impurities are discussed. Section 5 considers the mutual interactions between equilibrium defects and impurities, especially in relation to diffusion phenomena and generation of stacking faults. Section 6 is devoted to the study of the most important extended defect of single-crystal silicon—the surface. Because of its technological relevance, emphasis is concentrated upon the Si–SiO_2 interface. Section 7 is devoted to the techniques which preserve the surface region free from impurities and extended defects.

1. Silicon as a solvent

1.1. *Diamond-cubic silicon*

Until recently, silicon was presumed to have only one crystal structure—diamond-cubic (Cotton and Wilkinson 1980). The diamond-like structure of silicon is face-centred cubic (f.c.c.) with two atoms per unit cell; the lattice constant a is 5·431 Å and the atomic density N_{Si} is $5{\cdot}0 \times 10^{22}\,cm^{-3}$. From the topological point of view, in diamond-cubic (d.c.) crystals the ring, i.e., the closed path around the atom, of minimum size is six-membered, not planar and of the 'chair' type. Because of the impossibility of representing in a plane six-fold rings where each vertex has a tetrahedral coordination, our two-dimensional (2D) representation of the d.c. lattice will be a square lattice, so preserving stoichiometry.

The energy gap E_g is 1·17 eV at 0 K and charge screening effects take place via a large relative dielectric constant ε_{Si} ($\varepsilon_{Si} = 11{\cdot}7$ in the static limit). Extensive data of mechanical, thermal, optical and electrical properties of silicon are reported in Wolf (1969) *Silicon Semiconductor Data.*

Recent experiments on hydrostatically compressed d.c. silicon have shown the existence of two other phases—the β-tin and the simple hexagonal. The existence

† Present address: EniChem, Via Medici del Vascello 26, 20138 Milano MI, Italy.

regions and the energy contents of these phases can be determined theoretically with quantum-mechanical calculations (Yin and Cohen 1980, 1982, Yin 1985). Excellent agreement exists between experimental findings and theoretical predictions. For the wurtzite-like hexagonal phase of silicon, which is theoretically described as a metastable phase with a small energy excess ($\approx$0·01 eV/atom), experimental evidence has been given for anvil indentation at temperatures around 600°C (Eremenko and Nikitenko 1972) and ion implantation in the high-current, high-temperature (> 200°C) mode (Tan *et al.* 1981, Cerofolini *et al.* 1984).

1.2. *Amorphous silicon*

Several layers, referred to as 'amorphous', have been obtained and studied. The properties of the layer depend strongly upon the preparation technique—glow discharge, evaporation, chemical vapour deposition and ion implantation give rise to different amorphous layers. In this work we only consider the amorphous silicon (a Si) obtained by ion implantation (I^2).

Before considering the nature of amorphous layers which can be obtained by ion implantation, we give a short discussion of the mechanisms through which the ion (usually with an atomic weight A in the range 10–100 and energy E in the range 20–200 keV) loses its energy. Energy loss takes place by collisions with electrons (electronic energy loss) and with atoms (nuclear energy loss). Energy lost by collisions with electrons is quickly transformed into heat, while the energy lost by collisions with silicon atoms is responsible, in our view, for the following phenomena (Meda *et al.* 1987).

(1) If the collision has a high impact parameter, the transferred energy is low (say, < 10 eV) and the displaced target atom transfers its energy excess to the neighbouring atoms in the form of vibrations, so that lattice regularity is eventually preserved.
(2) If the collision has a low impact parameter, the transferred energy is moderately high (say, in the range 30–300 eV) and the recoiled atom remains at the end of the process permanently off-site, so leaving a lattice vacancy.
(3) If the collision has a low impact parameter, the transferred energy is high enough to generate a collisional cascade (tentatively > 1 keV); in turn the collisional cascade originates a hot cloud which, if sufficiently hot (i.e. for transferred energy higher than 5 keV), results after quenching in an island of displaced atoms.

1.2.1. *Amorphous 1*

It is reasonable to admit that displaced atoms remain off site only if a relevant number of neighbouring atoms are involved in such a displacement. This event occurs with higher probability at a depth variable with the implant energy, between the surface and a fraction, say 80%, of the projected range R_p of the ion in silicon (Prussin 1985).

For displacement events independent of one another, the expected number of displaced atoms per unit area, N_{dis}, should increase less than linearly with fluence Φ up to a critical fluence Φ_c and then saturate when all atoms are displaced. Actually, experiments studying the early stages of damage release show a superlinear increase of N_{dis} with Φ, this phenomenon being more evident the lighter the implanted ion (Thompson *et al.* 1980). This superlinear increase is easily understood by observing that it is easier to amorphize an already damaged crystal than an undamaged one; obviously, this explanation contradicts the hypothesis of independent events.

Table 1. Amorphization fluence for B, P, As and Sb.

Ion	E/keV	R_p/nm	Φ_c/cm^{-2}	Reference
B	25	82	9×10^{15}	Our datum
P	90	110	3×10^{14}	Prussin (1985)
As	150	85	8×10^{13}	Our datum
As	190	106	8×10^{13}	Prussin (1985)
Sb	80	38	1×10^{14}	Our datum

The critical fluence Φ_c depends weakly on the implant energy E (provided that E is high enough), but very strongly upon ion mass. Table 1 collected some experimental values of Φ_c for boron, phosphorus, arsenic and antimony projectiles for implantations at room temperature. Once a thin layer is completely amorphized, an increase of fluence is responsible for an extension of the damaged region both in depth and toward the surface.

Consider now an implant at a fluence just above Φ_c. In this situation a layer of thickness x_{dis} centred before R_p is amorphous, and the number of vacancy–self-interstitial pairs created is given by $y_{vi}\Phi_c$, where y_{vi} is the yield for such events. Taking this yield of the order of 10, and considering that such defects are spread over a region of the order of $2R_p$ (Mazzone 1985), provided that the implanted ion is heavy enough (e.g. As), Φ_c is low and the concentration of vacancies and self-interstitials is small compared with the silicon atomic density N_{Si} (say, 10^{19} cm^{-3} versus 5×10^{22} cm^{-3}). In this situation the amorphous appearance cannot be ascribed only to point-like defects and must be thought of as due to atoms displaced from their lattice location. We think that in this amorphous phase, referred to as a_1, the d.c. topological order is preserved, i.e. bonds are distorted but not broken.

The idea that the amorphous phase retains the same topological order as the phase from which it was obtained by low-temperature ion implantation, is upheld by the following Paradigm: *If the silicon phase X is stable to heat treatments comparable to the one of annealing at temperature* T *and to the one responsible for amorphization, then*

$$\forall X : X \xrightarrow{I^2} a_1 \xrightarrow{T} X$$

This statement was proven by taking X = d.c. Si, and X = (220) preferentially oriented poly-silicon (Cerofolini *et al.* 1987).

Two other pieces of evidence suggesting that the amorphous phase obtained by ion implantation retains memory of the crystalline phase are the ones by Geddo *et al.* (1986), showing by electroreflectance that one specific structure (E_1) of the interband spectrum of silicon (witnessing for crystal order) survives up to complete amorphization, and by Servidori *et al.* (1987), showing the ion-implanted amorphous phase can be thought of as containing vacancies and self-interstitials, thus witnessing for at least topological order. Preservation of bonds, though distorted, is favoured by the strongly covalent nature of silicon, and the relative weight of the second recoil event with respect to the third depends upon the mass and energy of the impinging atom. If its mass is high enough (e.g. arsenic in silicon), crystal order can be destroyed (however,

preserving topological order) much before a relevant concentration of vacancy-interstitial pairs is formed.

The transition from the a_1 phase to the d.c. one does not require bond breakdown but simply atom rearrangement, so that the a_1 layer can be reconstructed by heat treatments at moderate temperature $>450°C$. The reconstruction process, known as solid phase epitaxy (SPE), starts at the undamaged bulk seed, is thermally activated (the activation energy of about 2·5 eV being necessary to transport off-site atoms to their lattice locations) with a pre-exponential factor of the order of the sound velocity (Csepregi *et al.* 1977). This coincidence upholds the idea that the topological order in a_1 Si is the same as in d.c. Si.

When the fluence increases, the number of v-i pairs produced increases monotonically with Φ, eventually reaching a value not negligible with respect to N_{Si} (say, a few percent). This situation is characterized by a vacancy excess close to the surface and a self-interstitial excess in depth.

If the implant takes place on substrates kept at relatively high temperatures, vacancies and self-interstitials generated in pairs during the implant migrate and partially recombine, and displaced atoms return to their equilibrium positions (Csepregi *et al.* 1976). Implants at these temperatures result in the formation of partially reconstructed silicon (Csepregi *et al.* 1976, Cerofolini *et al.* 1985 a), the residual damage being formed by: dislocation segments, twins, stacking faults and rod-like hexagonal defects. This damage does not reconstruct by SPE; at temperatures above 1100°C, strongly damaged silicon melts and the crystal can be reconstructed by liquid phase epitaxy starting at the undamaged bulk seed, the activation energy for this process being about 4·5 eV.

1.2.2. *Amorphous 0*

An amorphous layer obtained by melting silicon and quenching it, without an underlying seed, is completely different from the amorphous phase obtained by ion implantation. In fact, this sudden quenching leads to a state of supercooled liquid with no topological order (Campisano *et al.* 1985). This phase is the structure which is more easily modelled by current theories.

Other amorphous layers (referred to as a_0) are obtained by glow discharge from SiH_4; these phases are characterized by a dangling bond density of the order of $10^{19}\,cm^{-3}$ which can be passivated by reaction with hydrogen. Table 2 collects the thermodynamic properties of these phases. To fill this table we have taken the energy excess of the a_1 phase from Donovan *et al.* (1983, 1985) and of the a_0 phase from Fan and Andersen (1981).

Table 2. Thermodynamic properties of silicon phases.

Phase	Stability/°C	Energy excess/eV	Order
d.c.	1417	0	Crystalline
a_1	450	0·13	Topological
a_0	$\simeq 1100$	0·12	None

2. Equilibrium defects

Equilibrium defects are lattice defects whose existence is thermodynamically guaranteed by the finite non-zero temperature of the lattice. These defects are therefore characterized by an equilibrium concentration. Although some equilibrium defects disappear in the thermodynamic limit, e.g. surfaces, they can play a fundamental role in determining the concentration of defects which do not disappear in the thermodynamic limit, e.g. vacancies, self-interstitials and their clusters. In fact, a mechanism through which equilibrium defects are generated is just surface reconstruction.

For a process at constant pressure, the equilibrium atomic density N_x of the point defect x (x = v, vacancy; i, self-interstitial; ...) at absolute temperature T is given by

$$N_x/(N_x^0 - N_x) = \exp(-\Delta G_x/k_b T) \tag{1}$$

where N_x^0 is the atomic density of allowed sites for the defect x, ΔG_x is the formation Gibbs free energy of the defect, and k_B is the Boltzmann constant.

The number of allowed sites depends on the nature of the defect. For an infinite crystal, $N_v^0 = N_{Si}$, and presumably in all cases $N_x^0 \approx N_{Si}$. The same equation as (1) holds true for a process at constant volume, provided that ΔG_x is replaced by the Helmholtz free energy ΔF_x. These considerations hold true only for processes where all defects can be absorbed or injected independently of one another; in particular, they hold when surface reconstruction is possible. However, in most practical situations the sample surface is subjected to external constraints and, therefore, is not free to self-reconstruct. An example of constraint is given by an oxide layer, which forbids surface reconstruction because of the strength of the Si–O bonds.

Thus, together with processes at constant pressure or volume usually considered by thermodynamics, for equilibrium defects one must also consider the *process at constant surface*. Not only does this process keep constant the total area, but also leaves the shape unchanged, i.e. the distribution of various patches with extension $A_{[hkl]}$ and orientation $[hkl], \forall h, k, l: A_{[hkl]} = \text{constant}$. Such a process is characterized by the condition

$$\Delta N_v = \Delta N_i \tag{2}$$

where ΔN_x is the number of defects (x = v, i) injected (generated) by the process in addition to preexisting ones.

Condition (2) follows from the fact that, in the absence of surface reconstruction, vacancies and self-interstitials are necessarily generated in pairs; it holds true not only in equilibrium, but also for all processes where surface reconstruction is not allowed. We feel that some discrepancies in data on vacancies and self-interstitials among different authors are due to neglect of the influence of constraints forbidding surface reconstruction, an example being the native oxide layer usually present because of high silicon reactivity.

2.1. *Vacancy*

The vacancy is the lattice site associated with a missing atom. The missing atom leaves four dangling bonds which can form two pairs of molecular orbitals. In this case

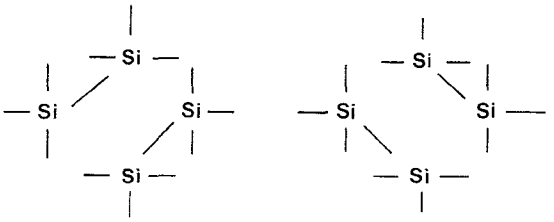

There is also the precondition for removing the electronic degeneracy through relaxation to a more stable configuration by a Jahn–Teller distortion (Watkins 1975). The major difficulties in the theoretical analysis of equilibrium defects come from relaxation phenomena, which might involve a relevant number of lattice atoms. The 'extended nature' of point-like defects, however, is still an open question (see the next two subsections).

The molecular orbitals formed by the superposition of dangling bonds are obviously strained and can be broken with relative ease by interaction with electrons or holes from the conduction or valence bands. After the interaction, the vacancy acquires a positive or negative charge, e.g.

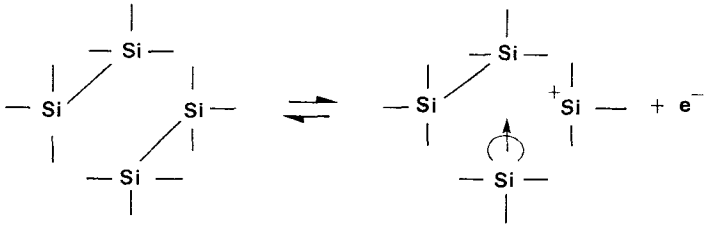

or, more schematically,

$$v^{\circ} \rightleftharpoons v^{+} + e^{-}$$

Four charge states of the vacancy have been hypothesized; these states and their trap behaviours are reported in table 3, though charge-state assignment of the electrical levels of the vacancy is still an unsettled question (Watkins 1979).

The equilibrium concentration of vacancies in silicon is much lower than in a metal. The qualitative reason for this is the following: the packing density of the diamond lattice is only 34% against 74% for a closed-packed structure such as the f.c.c. lattice of

Table 3. Charge states and trap behaviours of the vacancy.

Charge state	Trap behaviour
v°	Donor (0/+)
v^{-}	Acceptor (−/0)
$v^{=}$	Acceptor (− −/−)
v^{+}	

metals, e.g. copper and silver. Because of this geometrical condition, one expects that the incorporation of interstitial atoms in silicon is favoured, while the formation of vacancies occurs with difficulty. In passing, it is worthwhile noting that the very open structure of the d.c. lattice makes the a_1 configuration possible.

For vacancies, $N_v^0 = N_{Si}$; this property, however, is the unique one about which there is general agreement among different authors. For instance, decomposing ΔG_v into its enthalpy and entropy contributions, $\Delta G_v = \Delta H_v - T\Delta S_v$, Masters and Gorey (1978) give $\Delta H_v = 3{\cdot}66$ eV, $\Delta S_v = 7k_B$; the most recent theoretical calculations by Car *et al.* (1984) do not estimate the formation entropy and give a formation enthalpy of about 5 eV. The high experimental value entropy suggests that the vacancy has an extended nature. The problem of whether or not the vacancy has an extended nature has long been debated in the literature. For instance, in an early paper, Van Vechten (1974) suggested that the vacancy is a true point-like defect with a local octahedral structure, but in a recent paper (1985), he postulates the existence of extended vacancies. Seeger and Frank (1985), however, state that the latter model of the vacancy is not tenable to explain diffusivity in silicon.

We shall briefly discuss the idea of Van Vechten on extended vacancies. Since in the amorphous phase the energy excess is about 0·1 eV/atom, configurations with several (say, up to 40) displaced atoms should be energetically equiprobable with a single vacancy; such amorphous clusters could then arrange to form extended vacancies or self-interstitials. The last possibility can actually occur only if topological order in the amorphous cluster is not preserved, and the fact that extended vacancies seem not to exist upholds our view of the a_1 phase.

2.2. *Self-interstitial*

No generally accepted model of silicon self-interstitial is known. We recall here only the early view of the self-interstitial as an almost-free silicon atom embedded in the silicon matrix (James and Lark-Horovitz 1951)

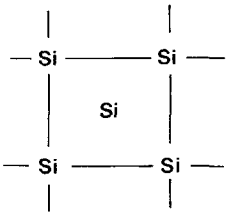

and the more recent view of the self-interstitial as a pair of silicon atoms in a dumb-bell configuration upon a lattice (Frank 1975):

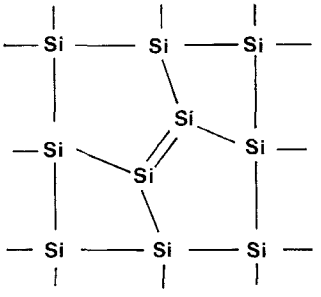

In the dumb-bell configuration the double bond can easily be opened thus forming the ionized self-interstitial, e.g.

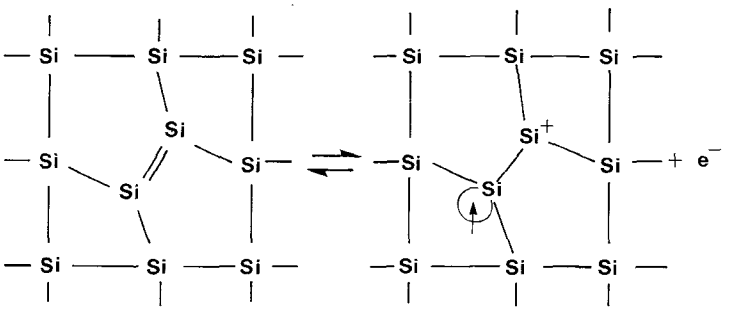

or, in short

$$Si_i \rightleftharpoons Si_i^+ + e^-.$$

The self-interstitial is characterized by negative and positive charge states with energy close to the midgap, showing the amphoteric nature of the self-interstitial.

Thermodynamic data for the self-interstitial suffer from the same difficulties as for the vacancy. First, the number of allowed sites depends upon the assumed structure of the defect. Second, the self-interstitial seems to have an extended nature. This conclusion is obtained by inspection of table 4, giving the formation entropy and enthalpy of the self-interstitial (Mayer *et al.* 1977). The high value of the formation entropy at high temperature suggests that in these conditions the disorder is spread upon many silicon atoms. Taniguchi *et al.* (1983) studied the growth of stacking faults in the temperature range 1100–1200°C and estimated completely different values (a formation enthalpy of 0·7 eV/atom and a negative formation entropy of $-7{\cdot}6k_B$), but paradoxically their results (the large negative formation entropy) lead to the same conclusion of the extended nature of the self-interstitial. More recently, Bronner and Plummer (1984) reconsidered the same problem, confirmed the negative formation entropy (although much larger, $-26k_B$), but obtained a high formation enthalpy. Third, to conclude this subsection, we note that extended theoretical calculations (Car *et al.* 1984, Pantelides 1984) give a formation enthalpy around 5 eV without indications on the formation entropy.

Table 4. Formation entropy and enthalpy of the self-interstitial.

T/K	$\Delta S_i/k_B$	ΔH_i/(eV/atom)
570	1	2·6
1320	5·02	2·90
1658	6·11	3·04

2.3. *Vacancy—self-interstitial pair*

We have already observed that when surface reconstruction is impossible, the vacancy and self-interstitial cannot be generated independently, but are formed simultaneously. We give what we believe is evidence for this mechanism in section 5.2.2. We also feel that some discrepancies among different authors concerning vacancies and self-interstitials are actually due to having neglected their generation in pairs. Once

generated in pairs, vacancies and self-interstitials can migrate, giving rise to two free defects, or can remain adjacent, for instance because they are electrostatically stabilized in the ionized forms v^+i^- or v^-i^+. It is not precisely known if such pairs exist or in which ionized state; what seems sure is that a barrier exists against their recombination. For this barrier, both enthalpic (Wertheim 1959, Hu 1977) and entropic (Gösele *et al.* 1982) natures have been postulated.

The entropic nature is easily understood if one admits that the self-interstitial, and possibly the vacancy, are spread out over several atomic volumes. According to Gösele *et al.* vacancy-interstitial recombination requires the contraction of both defects to about one atomic volume at about the same location. Since the number of microstates associated with extended defects is larger than the number of microstates of the point defect, the contraction requires a decrease of entropy, i.e. an entropy barrier.

Though the v-i pair is presumably stable, its formation enthalpy ΔH_{vi}, being the sum of the formation enthalpies of a vacancy and a self-interstitial, should be in the range 4–8 eV. The density of pairs which form under equilibrium conditions for a process at constant surface is given by (Kittel 1976)

$$N_{vi}^2/(N_v^0 - N_{vi})(N_i^0 - N_{vi}) = \exp(-\Delta H_{vi}/k_B T) \tag{3}$$

where all entropic contributions have been ignored. Taking $N_i^0 \simeq N_v^0 = N_{Si}$, for $N_{vi} \ll N_{Si}$, equation (3) is reduced to

$$N_{vi} \simeq N_{Si} \exp(-\Delta H_{vi}/2k_B T)$$

Assuming that $\Delta H_{vi} = \Delta H_v + \Delta H_i$, the concentration of defects formed in a process at constant surface is controlled by a formation enthalpy $(\Delta H_v + \Delta H_i)/2$ and then is much lower than the concentration of defects formed in a process at constant volume or pressure, which is controlled by the lowest enthalpy. However:

vacancy and self-interstitial can exist as a close pair, because of their recombination enthalpy or entropy barrier;
vacancy and self-interstitial can exist as an ionized pair irrespective of the Fermi energy, because of their amphoteric natures;
according to the value of the Fermi energy, different ionized pairs (v^+i^- or v^-i^+) can be obtained;
with respect to a pair formed by infinitely separated ionized vacancy and self-interstitial, the close pair requires a lower formation energy, the difference being equal to the Coulomb attractive energy in the absence of lattice reconstruction;
if in the close pair the v–i distance is less than one lattice distance, the dielectric constant screening the Coulomb interaction may be assumed to be the vacuum one, giving an attractive energy of the order of 4 eV; and
the vacancy or the self-interstitial can leave the close pair by replacement with an ionized impurity, e.g. v^- can leave the v^-i^+ pair by interaction with an ionized acceptor, such as B^-.

In conclusion, the close ionized v–i pair may be considered as a native defect with a modest formation enthalpy ($\frac{1}{2}\Delta H_{vi} = 2-4$ eV) and can be formed everywhere in the crystal irrespective of the possibility of surface reconstruction.

2.4. *Stacking faults*

Vacancies and self-interstitials can be present even in non-equilibrium concentrations. For instance, an excess of both can be obtained by quenching a sample

after high-temperature annealing; an interstitial excess and a vacancy deficiency within a few diffusion lengths from the $Si–SiO_2$ interface can be obtained during silicon oxidation below 1200°C.

2.4.1. *Extrinsic stacking fault*

When these defects are in large excess with respect to their equilibrium concentration, they can precipitate in a metastable phase. Self-interstitial precipitates in discs lying on (111) planes are referred to as *extrinsic stacking faults* (ESFs). Precipitation in (111) planes is a probable process (but not unique· (113) defects are also known (Desseaux-Thibault *et al.* 1983)) because the energy excess is quite small, of about 50–60 erg/cm^2 (Ray and Cockayne 1971, Föll and Carter 1979); this small energy difference comes from the third nearest neighbour arrangement, so that the system is only slightly disturbed compared to other bond-breaking defects, such as dislocations (Chou *et al.* 1985). Figure 1 shows the scanning electron microscope (SEM) view of the etch pattern after Secco etching† of an ESF starting at the $Si–SiO_2$ interface and due to a self-interstitial excess generated by oxidation. Precipitation into stacking faults requires a self-interstitial excess and is greatly favoured by nuclei for precipitation. These nuclei are often at the surface and several techniques have been proposed for their reduction (see Section 7.1).

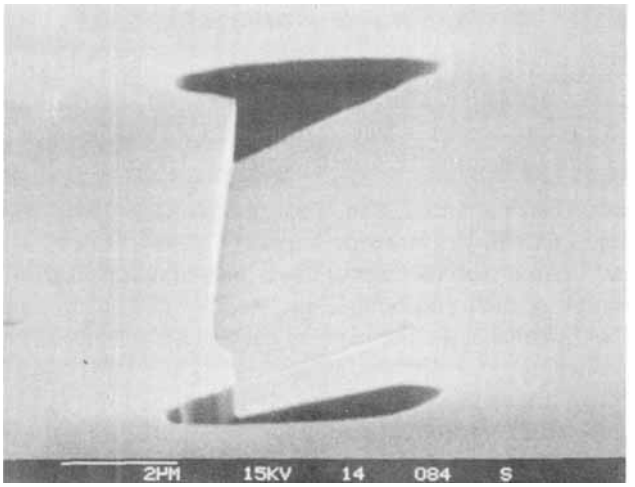

Figure 1. Scanning electron microscope view of the etch pattern after Secco etching of a (111) ESF. The etch puts in evidence the extra plane and the bordering dislocation loop.

2.4.2. *Intrinsic stacking fault*

The *intrinsic stacking fault* (ISF) can be seen as a precipitate of vacancies or, equivalently, as a missing disc of silicon atoms in a (111) plane. Though its energy excess should be of the same order as that of the ESF, in a recent review Zulehner and Huber (1982) claimed that 'up to now [1982] no intrinsic stacking fault that has been formed by vacancy agglomeration has been detected in silicon, only extrinsic ones'. Later,

† Secco etch is a concentrated $HF + Na_2Cr_2O_7$ aqueous solution which preferentially etches highly stressed regions, thus giving evidence for extended defects (Secco D'Aragona 1972).

however, Claeys *et al.* (1984) gave transmission electron microscope (TEM) evidence for an ISF, while Cerofolini and Polignano (1984) suggested that ISFs and ESFs can be formed simultaneously during oxygen precipitation, and supported this hypothesis with SEM evidence (see Section 5.2.2). ISFs are also formed after annealing in implanted layers close to the surface, where a vacancy excess is created because of recoil effects (Polignano *et al.* 1986). Interestingly enough, ISFs have been observed mainly in situations where oxygen plays a large role. It is possible that the ISF can exist only in these situations.

First-principle calculations of the energy excess of stacking faults give 26 erg/cm^2 for the ESF and 40 erg/cm^2 for the ISF (calculated by Chou *et al.* (1985) in the hypothesis that the ISF actually does not involve broken bonds). These calculations suggest that ISFs should form easily; the rarity of ISF observations indicates that some hypotheses under which the formation energy was calculated is false.

3. Impurities

While intrinsic defects are formed simply by thermodynamic reasons and can be controlled by prolonged annealing, impurities (which may be present in silicon even at high concentrations because of the growth technique) cannot usually be removed by simple heat treatments. Impurities come from the ingot preparation process (and in this case are often unwanted) or can be inserted by doping.

Table 5 lists the major impurities in semiconductor silicon; Group III and V elements are considered extensively in the next section; heavy metals are considered in Section 7; this section is devoted mainly to oxygen.

Table 5. Major impurities in silicon.

Elements	Source	Lattice location	Diffusivity
Group III–V ('dopants')	Ingot or doping	Substitutional	Very slow
Group IV (except C)	Doping	Substitutional	Very slow
Carbon	Ingot	Substitutional	Very slow
Metals	Ingot (unwanted) or doping	Interstitial	Fast
Oxygen	Ingot	Interstitial	Slow

3.1. *Impurity content in relation to the growth technique*

Impurity content in silicon depends rather markedly on the growth technique. Commercial single-crystal silicon is produced either by the Czochralski (CZ) method or by the float zone (FZ) method. These methods are briefly described by Herrmann *et al.* (1975); more details on the CZ method are given by Zulehner and Huber (1982).

Table 6 reports the typical oxygen and carbon content for FZ and CZ crystals; for comparison, solid solubilities at 1200°C are also reported (Kolbesen and Mühlbauer 1982). The comparison shows that carbon concentration may exceed solid solubility both in CZ and FZ crystals, while oxygen concentration may exceed solid solubility only in CZ crystals. The CZ technique is usually preferred in semiconductor technology because a higher oxygen content is responsible for an increase of the plastic limit τ. This quantity is defined as the maximum stress below which deformation remains elastic; stresses larger than τ are plastically absorbed by the crystal through the formation of dislocations. Since dislocations cause severe deviations from ideal behaviour of electronic devices, care is taken to avoid them.

Table 6. Oxygen and carbon content in single-crystal silicon.

Growth	[Oxygen]/cm^{-3}	[Carbon]/cm^{-3}
FZ (vacuum)	$<3\times10^{15}$	$<5\times10^{16}$
FZ (argon)	$<2\times10^{16}$	$<3\times10^{17}$
CZ	4×10^{17}–2×10^{18}	10^{16}–5×10^{17}
Solid solubility at 1200°C	5×10^{17}	5×10^{16}

Figure 2, taken from Kondo (1981), compares the plastic limits of CZ and FZ materials at different temperatures; the comparison shows that the plastic limit of the CZ crystal is higher than that of the FZ crystal, the relative difference being greater the higher the temperature. Since dislocations can form only in high-temperature heat treatments, the previous comparison suggests the use of CZ crystals at least in integrated circuit manufacturing.

Table 7 reports the properties of CZ silicon (Zulehner and Huber 1982); however, different producers have slightly different specifications on impurity content (compare tables 6 and 7); the data on diameter, however, are already oldish and slices of 155 mm are commercially available.

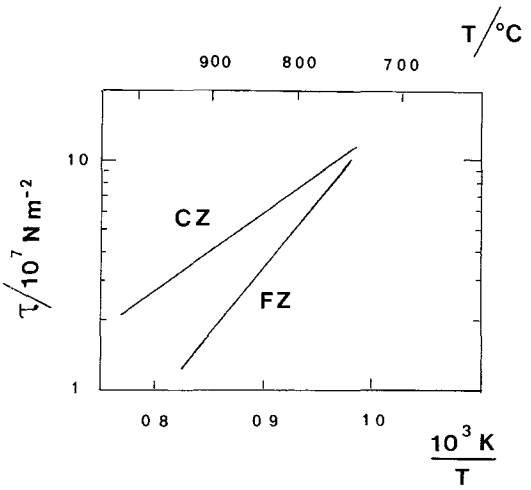

Figure 2. Comparison of plastic limits of CZ and FZ materials at different temperatures.

3.2. *Oxygen*

Oxygen in CZ silicon comes from the reduction of crucible SiO_2 by molten silicon

$$Si + SiO_2 \rightleftharpoons 2SiO\uparrow;$$

SiO, in turn, is incorporated in the melt and hence in the ingot; for more details, see Zulehner and Huber (1982).

Table 7. Properties of Czochralski-grown silicon single crystals.

Quality	Producible	Commercial
Diameter (mm)	Up to 160	50–100
Length (mm)	Up to 2200	500–1600
Weight (kg)	Up to 48	5–25
Orientations	⟨100⟩, ⟨111⟩, ⟨110⟩, ⟨511⟩	⟨100⟩, ⟨111⟩
Dopant concentration (cm^{-3})		
Boron	10^{14}–10^{20}	2×10^{14}–10^{20}
Phosphorus	10^{14}–6×10^{19}	10^{14}–7×10^{17}
Antimony	10^{14}–2×10^{19}	10^{18}–10^{19}
Arsenic	10^{14}–8×10^{19}	5×10^{18}–8×10^{19}
Aluminium	10^{14}–5×10^{17}	Not standard
Gallium	10^{14}–10^{18}	Not standard
Indium	10^{14}–$1{\cdot}5\times10^{16}$	Not standard
Impurity concentration (cm^{-3})		
Carbon	$<10^{16}$ by selection	$<5\times10^{15}$–5×10^{16}
Oxygen	2×10^{17}–2×10^{18}	5×10^{17}–$1{\cdot}4\times10^{18}$
Crystal defects		
Dislocations	Free	Free
Precipitates	Free	Free

Oxygen in silicon holds an interstitial position bridging two nearest-neighbour silicon atoms:

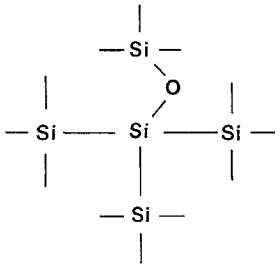

Because of symmetry considerations, 24 equivalent sites are possible. Though oxygen holds interstitially, its diffusivity is not comparable with the one of interstitial metals because of the covalent nature of the Si–O bond; the dependence of the diffusion coefficient on temperature is given by Oherlein and Corbett (1983) as

$$D_{O_i}=0{\cdot}16\exp(-2{\cdot}53\,\mathrm{eV}/k_BT)\,\mathrm{cm}^2/\mathrm{s}.$$

Since in CZ crystals the oxygen concentration usually exceeds the solubility, oxygen precipitation can occur. Precipitation takes place via formation of clusters where a silicon atom is tetrahedrally bound to four oxygen atoms as in SiO_2:

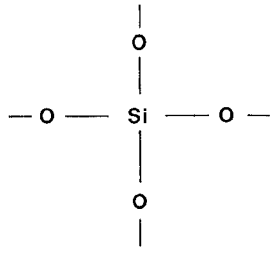

The interface between silicon and precipitated SiO_2 will be characterized by broken, unsaturated or deformed bonds so that it will presumably behave as a generation-recombination centre for electrons and holes.

Oxygen precipitation is responsible for the transformation of a silicon volume V_{Si} into a precipitate volume V_{SiO_2}. Since $V_{SiO_2}/V_{Si} \approx 2$, oxygen precipitation puts the silicon crystal in a compressive state which, if the cluster is large enough, can be relieved by emission of self-interstitials. If precipitated SiO_2 is in the same compressive state as thermally grown SiO_2, the number x of self-interstitials injected per precipitated molecule is of the order of unity ($x \approx 1$):

$$(1+x)\mathrm{Si} + 2\mathrm{O_i} \rightleftharpoons \mathrm{SiO_2}\downarrow + x\mathrm{Si} \qquad x \approx 1. \tag{4}$$

This view (Plougoven *et al.* 1978) is perhaps over-simplified (Hu 1986) and will be discussed further in Section 5.2.2.

Kinetics of oxygen precipitation are very complex and may occur homogeneously or heterogeneously on pre-existing nucleation centres. Hu (1981) has suggested that vacancy clusters may be active nucleation centres for oxygen precipitation. Hu showed that oxygen precipitation is retarded by an anneal in oxygen compared with an anneal in nitrogen atmosphere, which can be interpreted by admitting that the interstitial excess generated during oxidation diffuses into the bulk and annihilates the vacancy clusters.

Irrespective of the detailed mechanisms through which oxygen precipitation occurs, this phenomenon can take place at temperatures high enough to allow oxygen diffusion, but low enough to permit over-saturation. Since the solid solubility increases with temperature, in practice oxygen precipitation does not occur for processes at temperatures above 1250°C. For lower temperatures, in the range 800–1200°C of interest for semiconductor device processing, precipitation occurs in relation to: temperature, interstitial oxygen concentration and silicon thermal history (responsible for precipitation nuclei). More details on the control of oxygen precipitation are given in Section 7.2.

Interstitial oxygen at temperatures around 450°C or 850°C produces complexes known as *thermal donor* or *new thermal donor*, respectively. Extended data on kinetics of formation/destruction of thermal donors and new thermal donors are reported by Cazcarra and Zunino (1980).

3.2.1. *Thermal donor*

The thermal donor is a defect formed by heat treatments around 450°C and destroyed at temperatures above 550°C. The thermal donor is schematically characterized by two donor energy levels, at about 70 and 150 meV from the conduction band, and surely involves oxygen, as its kinetic features indicate:

the initial formation rate varies as $N_{O_i}^4$;
the maximum donor concentration varies as $N_{O_i}^3$;
the activation energy for the direct reaction equals that for the reverse reaction.

Several models have been proposed to explain phenomena involving thermal donors. For instance, and mainly to give an idea of the different arguments which have been advocated to explain the nature of thermal donors, we briefly mention three models often referred to in the literature.

The oldest one, due to Kaiser *et al.* (1958), explains all kinetic behaviour irrespective of the microscopic nature of the centre. This model assumes that:

(*a*) the formation of Si_mO_n complexes (*m*, *n* integers) occurs through consecutive addition of interstitial oxygen atoms,

$$Si_mO_n + O_i \rightarrow Si_mO_{n+1}$$

(*b*) the thermal donor requires the addition of four interstitial oxygen atoms;
(*c*) the addition of more oxygen atoms destroys the thermal donor.

In the Kaiser *et al.* model the thermal donor is a cluster with a definite, though unspecified, chemical composition $Si_mO_{\bar{n}}$ ($\bar{n} \geqslant 4$).

A suggestion about the nature of this centre was proposed by Oehrlein and Corbett (1983). Complexes such as Si_3O_2, Si_4O_3 and Si_5O_4 are assumed to be present after a certain anneal at 450°C. If the complex is not large, it stresses the crystal but with an energy which is insufficient to generate a self-interstitial (see, however, Section 5.2.2). Thus both silicon and cluster are compressed, and one can presume that in some conditions the strain is large enough to severely distort Si–O–Si bond angles thus causing a superposition of two lone 2p oxygen orbitals. The two interacting lone-pair orbitals result in bonding σ and antibonding σ^* molecular orbitals, while non-interacting 2p orbitals presumably remain unchanged. It suffices therefore to admit that the σ^* antibonding orbitals are in the conduction band to explain the double donor behaviour of the thermal donor:

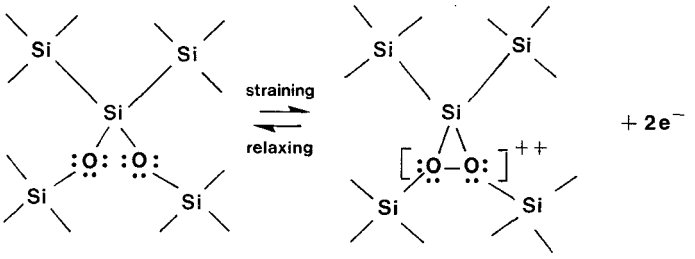

Larger clusters have an elastic energy sufficiently high to inject a self-interstitial into the crystal, thus relieving the stress and inactivating the centre.

The Kaiser *et al.* model was criticized by Helmreich and Sirtl (1977) on the grounds that the growth rate of the cluster, calculated from the diffusion coefficient of interstitial oxygen at 450°C, is too low compared to the thermal donor generation rate. To avoid this difficulty, Helmreich and Sirtl hypothesized a fast-diffusing form of interstitial oxygen, paired with a vacancy, and assumed the v–O_i pair as the thermal donor. This model is still considered (Rava *et al.* 1981), though quantum-mechanical calculations indicate that the v–O_i centre should be an acceptor, not a donor (Watkins and Corbett 1961).

Another model for the thermal donor was proposed by Gösele and Tan (1982) to explain the high oxygen diffusivity at 450°C. This model is based on assumptions that:

(*a*) interstitial oxygen atoms react to give a gas-like O_2 molecule embedded in the crystal, $O_i + O_i \rightleftharpoons O_2$;
(*b*) two oxygen molecules react to give a molecular complex O_4, $O_2 + O_2 \rightleftharpoons O_4$;

(*c*) the complex O_4 is the thermal donor; and
(*d*) the addition of O_i to O_4 inactivates the complex.

The above description does not exhaust all the proposed models of thermal donors; a recent review is given by Boûrret (1985).

3.2.2. *New thermal donor*

The new thermal donor was discovered only recently (Kanamori and Kanamori 1979); it is obtained after prolonged heating in the range 550–900°C and is not destroyed by heating to 1000°C (Cazcarra and Zunino 1980). The centre is surely related to both oxygen and carbon content, but no model has yet been accepted for it. Table 8 (Matsushita 1985) compares the properties of the thermal and new thermal donors.

Table 8. Characteristics of oxygen-related donors.

Quantity	Thermal donor	New thermal donor
Formation temperature	400–550°C	550–900°C
Donor killer	Heat treatments at 600–800°C	?
Generation rate	Fast	Slow
Oxygen concentration	High⇒fast	High⇒fast
Carbon concentration	High⇒slow	High⇒slow
Pre-heating		450°C pre-heating⇒fast
Energy level	70 meV, 150 meV	17 meV
Model	Si_mO_4 ($m \simeq 2$–3); O-v; O_4	?

4. Electronic properties of dopants

Impurities of Groups III and V play a fundamental role in the electronic properties of silicon and are usually referred to as *dopants*. Dopants of Groups III and V are *acceptors* and *donors*, respectively. The electronic properties of doped silicon are usually considered in the framework of a relatively simple theory—the *effective mass* approximation (EMA).

> EMA1, the dopant is tetrahedrally bound to 4 neighbouring silicon atoms;
> EMA2, the dopant is charged (positively if donor, negatively if acceptor) because the impurity is not isovalent with silicon;
> EMA3, the dopant charge, due to the tetrahedral configuration, causes a Coulomb potential which superimposes on the atomic potential generated by the distribution of valence and core electrons and by the nucleus; and
> EMA4, the interaction of a quasi-particle in the conduction or valence band with a dopant does not modify the quasi-particle (i.e. quasi-particle properties such as effective mass) so that the interaction is uniquely described in terms of dopant potential.

When the dopant satisfies conditions EMA1 to EMA4 it will be said to be *shallow*. *Mutatis mutandis*, the EMA can be applied to interstitial donors such as alkali ions.

4.1. *The standard theory of shallow dopants*

In the standard theory of shallow dopants (STSD), the quasi-particle is described by its unperturbed lattice properties. The band structure of silicon is characterized by a

band-gap $E_g = 1{\cdot}17$ eV at 0 K, with minima in the conduction band on values of quasi-momentum **k** directed along the ⟨100⟩ direction and maxima in the valence band at $\mathbf{k} = 0$.

Because of symmetry considerations, six equivalent valleys define the lowest-lying states in the conduction band; each valley is described by an anisotropic tensor m^*_{ik} $(i, k = x, y, z)$ with an ellipsoidal symmetry, the longitudinal effective mass being $m^*_{el} = 0{\cdot}97m_e$ and the transversal effective mass being $m^*_{et} = 0{\cdot}19m_e$, where m_e is the electron mass. The density-of-states effective mass, which takes into account the six valleys, is given by

$$(m^*_n)^{3/2} = 6(m^*_{el}m^{*2}_{et})^{1/2},$$

i.e. $m^*_n = 1{\cdot}1m_e$.

The valence band is described in terms of three holes: the *heavy hole*, with effective mass $m^*_{hh} = 0{\cdot}52m_e$; the *light hole*, with effective mass $m^*_{lh} = 0{\cdot}16m_e$, both with maxima at the top of the valence band; and the *split-off hole*, with effective mass $m^*_{soh} = 0{\cdot}16m_e$ and with maximum at 45 meV from the valence-band edge. For many considerations the split-off hole can be ignored and the four-fold degenerate dispersion law at quasi-momentum $\mathbf{k} = 0$ can be regarded as a unique quasi-particle with scalar effective mass

$$m^*_p = (m^{*3/2}_{hh} + m^{*3/2}_{lh})^{2/3} = 0{\cdot}58m_e$$

and spin $\frac{3}{2}$ (Wu and Falicov 1984).

In STSD a shallow dopant originates a Coulomb field screened by the silicon dielectric constant, the potential at a distance **r** from the dopant nucleus being

$$V_{coul}(\mathbf{r}) = -\frac{1}{4\pi\varepsilon_0\varepsilon_{Si}}\frac{ze}{|\mathbf{r}|} \tag{5}$$

where ε_0 is the vacuum permittivity, e is the positive unitary charge (SI units) and z is the net dopant charge ($z = 1$ for donors, $z = -1$ for acceptors). In addition to this potential, one must also consider the potential generated by the distribution of core electrons. However, if the guest dopant which replaces silicon is adjacent to it in the Periodic Table (i.e. aluminium and phosphorus in silicon, gallium and arsenic in germanium) the electron distributions of host and guest atoms are similar and potential (5) can be thought of as describing adequately the quasi-particle–dopant interaction.

4.1.1. *Hydrogen-like model*

The analysis of this interaction is particularly simple if the effective mass m^*_{ik} is a scalar m^*. In this case the eigenvalue problem for the quasi-particle is easily solved by scaling the result of the hydrogen atom, i.e. by replacing the electron mass m_e by m^* and ε_0 by $\varepsilon_0\varepsilon_{Si}$. This result follows from an accurate analysis of the problem, which shows that the *electronic* problem, i.e. the solution of the single-electron Schrödinger equation in the Coulomb potential superimposed with the crystal periodic potential, can be reduced to the Schrödinger equation for the *quasi-particle* in the Coulomb potential alone (Kittel and Mitchell 1954, Luttinger and Kohn 1955, Kohn 1957, Pantelides 1978).

In particular, the ionization energy E^*_{ion} and the radius of the ground-state orbitals a_* can be expressed in terms of the ionization energy of the hydrogen atom

E^{H}_{ion} ($E^{H}_{ion} = 13{\cdot}6\,eV$) and Bohr radius $a^{H}_{0} = 0{\cdot}5$ Å) as

$$E^{*}_{ion} = \frac{m^*}{m_e}\left(\frac{1}{\varepsilon_{Si}}\right)^2 E^{H}_{ion} \tag{6}$$

$$a_* = \varepsilon_{Si}\frac{m_e}{m^*}a^{H}_{0} \tag{7}$$

To estimate the orders of magnitude, taking $m^* = m_e$ we have $E^{*}_{ion} \simeq 100\,meV$ and $a_* \simeq 5$ Å.

It is obvious that the treatment is self-consistent only if a_* so exceeds the atomic radius of the impurity not to feel the details of the atomic potential.

Consider now the ionization energy E^{0}_{ion} of the hydrogen-like atom formed by the actual quasi-particle; because of band-structure complexity (resulting in an anisotropic tensorial effective mass for the electron and in a warped spin-$\frac{3}{2}$ particle for the hole), even large deviations of E^{0}_{ion} from E^{*}_{ion} are expected to occur. Sections 4.2 and 4.3 consider the problem of the real value of E^{0}_{ion}, which is still a lattice property independent of the dopant.

4.1.2. *Central cell correction*

The band-structure complexity is not the unique factor which may influence the ionization energy; the core electron distribution may be responsible for large deviations of the actual ionization energy of a given dopant E_{ion} from E^{0}_{ion}. The difference of the ionization energy of a dopant E_{ion} and E^{0}_{ion} will be defined as the *chemical shift* of the dopant. In general, the EMA admits a potential of the type

$$V(\mathbf{r}) = V_{loc}(\mathbf{r}) + V_{coul}(r) \tag{8}$$

where $V_{loc}(\mathbf{r})$ is the potential due to the electron distribution and responsible for the deviations of E_{ion} from E^{0}_{ion}. The *electron* eigenvalue problem for a potential of type (8) can be considered perturbatively and the solution is still expressed in terms of band properties, provided $V_{loc}(\mathbf{r})$ is confined within the first cell; in such a case one speaks of central cell correction (CCC) (Lannoo and Bourgouin 1981).

Irrespective of the details of the solution, we observe that if the potential $V_{loc}(\mathbf{r})$ is repulsive, then the correction to the ionization energy is small (in fact, a repulsive potential tends to localize the particle beyond the first cell, where by hypothesis $V_{loc}(\mathbf{r}) = 0$); values of E_{ion} much lower than E^{0}_{ion} are therefore incompatible with the CCC-EMA. In other words, large negative values of chemical shift cannot be explained by the EMA in the CCC.

4.1.3. *Equilibrium properties*

Hypotheses EMA1 to EMA4 are useful to determine the electronic properties of dopants. The STSD, however, is not exhausted at this stage but aims to describe equilibrium and transport properties also. To do this, STSD requires additional assumptions. For equilibrium properties they are as follows.

E1: Electron and hole densities, n and p can be varied by changing dopant concentration; however, their product np is a constant at constant temperature

$$np = n_i^2 \tag{9}$$

where n_i is the intrinsic concentration of electrons and holes, i.e. the concentration in the absence of any dopant, $n_i = (N_C N_V)^{1/2} \exp(-E_g/2k_B T)$, N_C and N_V are the density of states in conduction and valence band, respectively:

$$N_C = 2\left(\frac{2\pi m_e k_B T}{h^2}\right)^{3/2}\left(\frac{m_n^*}{m_e}\right)^{3/2},$$

$$N_V = 2\left(\frac{2\pi m_e k_B T}{h^2}\right)^{3/2}\left(\frac{m_p^*}{m_e}\right)^{3/2},$$

and h is the Planck constant.

E2: The ionization of neutral donors and acceptors is an equilibrium

$$A^- \ldots h^+ \rightleftharpoons A^- + h^+$$

$$D^+ \ldots e^- \rightleftharpoons D^+ + e^-$$

The equilibrium constant K is given by

$$K_D = \frac{nN_{D^+}}{N_D - N_{D^+}} = \frac{N_C}{g}\exp\left(-\frac{E_{ion}}{k_B T}\right) \tag{10}$$

$$K_A = \frac{pN_{A^-}}{N_A - N_{A^-}} = \frac{N_V}{g}\exp\left(-\frac{E_{ion}}{k_B T}\right) \tag{11}$$

where E_{ion} is the ionization energy, N_x denotes the concentration of the species x ($x = N_D, N_{D^+}, N_A, N_{A^-}$) and g is the degeneracy factor of the fundamental state: $g = 2$ for electrons because of spin-$\frac{1}{2}$ degeneracy, $g = 4$ for holes because of spin-$\frac{3}{2}$ degeneracy.

E3: The condition of local electroneutrality,

$$N_{D^+} - N_{A^-} + p - n = 0, \tag{12}$$

holds true everywhere.

If N_D and N_A are known, we have four equations (equations (9), (10), (11), 12)) in the four unknowns n, p, N_{D^+}, N_{A^-}, which can be solved, though not in a closed form. Therefore, hypotheses E1 to E3 allow the electron and hole concentrations to be calculated.

The above equations show that, for given N_D and N_A, hole and electron concentrations depend on the nature of the dopant only through their dissociation constant, i.e. through their ionization energy E_{ion}. It is interesting to remark that the equilibrium properties of electrons and holes are calculated in a way perfectly equivalent to the one used to calculate the dissociation properties of weak acids and bases in a dilute aqueous solution (Moore 1972). This analogy goes beyond the calculation of the ionized fraction, and the whole Debye–Hückel theory of ionic solutions can be restated for moderately doped semiconductors. The major difference is that dopants are considered immobile, i.e. N_D and N_A are given functions of position x. This analogy was noted in early works (Fuller 1956) and can be extended to find an analogy between the electrolytic cell and the p-n junction.

4.1.4. *Transport properties*

The motion of a quasi-particle under an external field is characterized by two regimes: *ballistic* and *dissipative.*

In the ballistic regime the particle moves under the action of the external force **F** alone. Its group velocity $\mathbf{v}_g$ is described in terms of Newton's second law:

$$\dot{\mathbf{v}}_g = \frac{1}{m_{ik}}\mathbf{F} \tag{13}$$

provided **F** satisfies suitable conditions (slow variation). In the absence of any scattering mechanism, under ballistic motion the quasi-particle seems in principle able to reach any wanted velocity.

Does a mechanism exist able to limit the velocity at most to the velocity of light c, internal to the theory itself? The answer is affirmative, as the maximum allowed group velocity w is given by the maximum of $|\mathrm{d}E/\mathrm{d}\mathbf{k}|$, where $E(\mathbf{k})$ is the dispersion relationship in the band; in turn w is a band property. To give an order of magnitude, for electrons in the conduction band $w \approx 6 \times 10^7$ cm/s (Solomon 1984).

In practice, however, high-field experiments show that the maximum drift velocity is limited to a value v_{sat} around 10^7 cm/s, quite irrespective of T in the range 4–300 K (Reggiani 1980). The interpretation is that the drift velocity is limited by other mechanisms not considered by the band description, i.e. scattering by phonons, ionized and neutral dopants.

When these mechanisms are present, the motion can no longer be viewed as ballistic, but becomes dissipative. In this regime, after a transitory period, for weak fields the drift velocity **v** becomes proportional to the external field. A particularly interesting case is that of the electric field $\mathbf{E}_{el}$; in this case, the constant of proportionality, μ, linking **v** to $\mathbf{E}_{el}$,

$$\mathbf{v} = \mu \mathbf{E}_{el}$$

is known as the mobility. In STSD the mobility is calculated with the following hypotheses (Nag 1972):

T1, the factor which limits the free motion of quasi-particles is scattering against (1) phonons, (2) ionized shallow dopants, and (3) neutral shallow dopants;
T2, these events are independent; and
T3, their statistical features are described by the Boltzmann transport equation in the relaxation-time approximation.

Under assumptions T1 to T3 the bulk mobility can be written as the harmonic composition of the lattice mobility μ_l (free motion limited by scattering on phonons, independent of dopant concentration), ionized impurity mobility μ_i (Rutherford scattering on ionized impurities), and neutral impurity mobility μ_n (scattering on neutral shallow dopants),

$$\frac{1}{\mu} = \frac{1}{\mu_l} + \frac{1}{\mu_i} + \frac{1}{\mu_n}$$

Models for the calculation of μ_l, μ_i, μ_n from first principles (band structure, scattering mechanisms and Boltzmann equation) are known (Nag 1972) and fit accurately experimental data for Si : B, Si : P and Si : As for dopant concentration below 10^{18} cm^{-3} in the temperature range 100–300 K (Larrabee *et al.* 1980). Experimental data for Si : In are much less accurately described by current theories (Cappelletti *et al.* 1982 a). Additional hypotheses are required to describe surface mobility, mobility in inversion layers or in poly-crystalline silicon.

4.2. *Group V donors*

Table 9 gives the ionization energies of Group V donors in silicon as given by Milnes (1973). The theoretical calculation of E^0_{ion} for electrons is a difficult task because of the tensorial nature of the effective mass in the conduction band. A way to deal with this problem is described, for example, by Pantelides (1978). Here it suffices to note that if we describe the conduction electron with a scalar effective mass $m^*_e = (m^*_{el} m^{*2}_{et})^{1/3} = 0{\cdot}32 m_e$, we have an ionization energy $E^*_{ion} \approx 30$ meV, while taking the density-of-states effective mass we have an ionization energy of about 100 meV. Inspection of table 9 shows that, neglecting nitrogen, the other donors have ionization energies around 50 meV; this value can therefore be assumed as representative of E^0_{ion}. This fact can be interpreted in the following way too: the electron anisotropy can simply be taken into account by defining another scalar effective mass m^{**}_e according to $m^{**}_e/m_e = \varepsilon^2_{Si}(E^0_{ion}/E^H_{ion})$ instead of m^*_e. In this way, the anisotropy of the quasi-particle is reduced to an effective-mass renormalization.

Table 9. Ionization energies of Group V impurities in silicon.

Element	E_{ion}/meV
N	140
P	44
As	49
Sb	39
Bi	69

The differences $E_{ion} - E^0_{ion}$ for all donors except nitrogen can be explained in terms of small chemical shifts (Morita and Nara 1966). For nitrogen the situation is more complex because the perturbation (the chemical shift) is higher than the unperturbed value (E^0_{ion}). It is therefore possible that in this case some of the basic assumptions of the EMA do not hold; for instance, it can be hypothesized that the neutral state of nitrogen is of the type

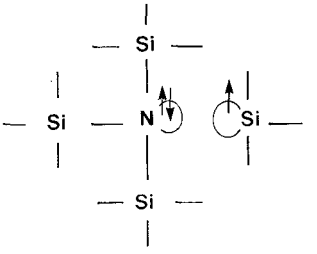

(the electronic configuration of nitrogen being as in ammonia); ionization should then involve a change of electronic configuration

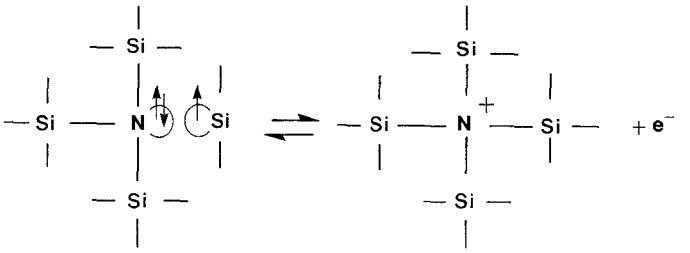

4.3. *Group III acceptors*

We have just seen how Group V impurities except nitrogen can be considered as shallow donors adequately described by a *scalar* EMA provided the electron effective mass is renormalized. The renormalized mass, $m_e^{**}=0{\cdot}5m_e$, explaining the observed ionization energies, is intermediate between the single-valley electron effective mass, $m_e^*=0{\cdot}32m_e$, and the density-of-states effective mass, $m_n^*=1{\cdot}1m_e$.

A similar procedure cannot be repeated for the hole (for instance, to deal with valence-band warpage) because the ionization energies of Group III elements vary greatly along the Periodic Table—from 44 meV for boron to 246 meV for thallium.

Table 10 collects the data of optical ionization energies of Group III acceptors as reported by Jones *et al.* (1981). The major conclusions of this section are not influenced by the small discrepancies among different authors on the last significant figure of E_{ion}.

The first idea to explain the values of E_{ion} for Group III impurities is due to Morgan (1970). In line with this idea, first we observe that an estimate of E_{ion}^0 on the grounds of a hole effective mass equal to the density-of-states effective mass ($m_p^*=0{\cdot}58m_e$) gives $E_{ion}^0=57$ meV. We compare (see table 11) the difference $E_{ion}-E_{ion}^0$ (tentatively, the chemical shift) of an impurity with its tetrahedral radius in silicon as given by Wolf (1969). This comparison shows that the difference $\Delta E=E_{ion}-E_{ion}^0$ is never negligible and has an interesting behaviour: (1) ΔE has the same sign as $r-r_{Si}$; (2) although the core electron cloud of Al ($Z=13$) is very similar to that of Si ($Z=14$), ΔE_{Al} is not negligible; (3) although the core electron clouds of Al and Ga ($Z=31$) are very different, $\Delta E_{Al}\approx\Delta E_{Ga}$; and (4) the tentative chemical shift increases with $r-r_{Si}$.

These facts show that the different impurities are discriminated mainly by their tetrahedral radii, and suggest that the chemical shift is associated with the energy required for straining the lattice. If this view is correct, the main contribution to ΔE must be elastic, i.e. it must increase roughly in proportion to $(r-r_{Si})^2$. Figure 3 supports this hypothesis. However, the idea of their elastic origin does not allow the observed chemical shifts to be explained by STSD. In fact, this problem can be considered in the

Table 10. Ionization energies of Group III impurities in silicon.

Element	E_{ion}/meV
B	44
Al	69
Ga	73
In	156
Tl	246

Table 11. Ionization energies, chemical shifts and tetrahedral radii of Group III acceptors in silicon.

Element	E_{ion}/meV	$(E_{ion}-E_{ion}^0)$/meV	r/Å	$(r-r_{Si})$/Å
B	44	−13	0·88	−0·29
Al	69	12	1·26	0·09
Ga	73	16	1·26	0·09
In	156	99	1·44	0·27
Tl	246	189	1·47	0·30

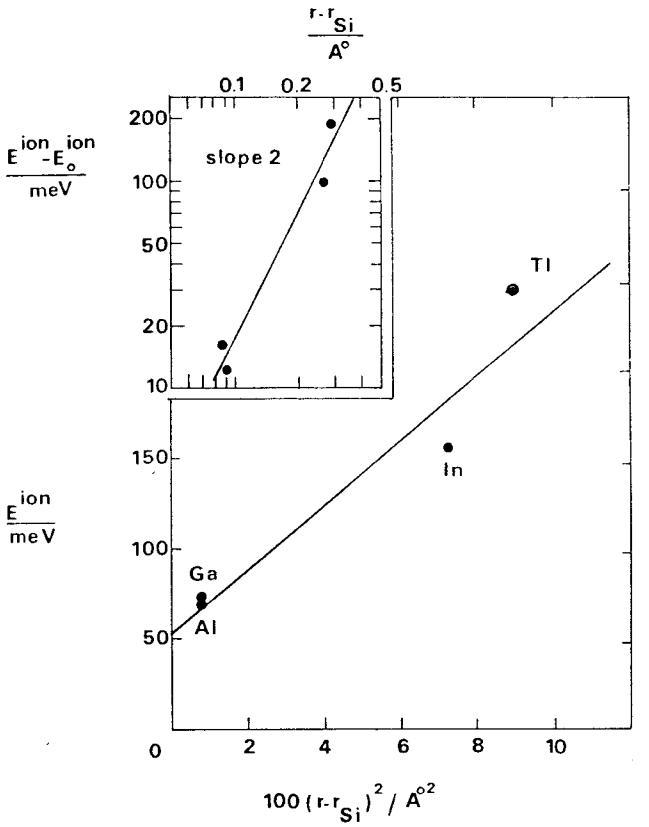

Figure 3. Linear and log–log plots of the ionization energy versus the tetrahedral radius. The log–log plot shows that the (supposedly existing) power law relating $E_{ion}-E^0_{ion}$ to $r-r_{Si}$ is quadratic; the plot of E_{ion} versus $(r-r_{Si})^2$ shows that the intercept at $r-r_{Si}$ practically coincides with the assumed E^0_{ion}, thus confirming this choice.

EMA by taking the deformation potential due to the difference of tetrahedral radii as a CCC. This problem can be solved, and the solution shows that even large differences of tetrahedral radii (up to 0·2 Å) are responsible for a modest chemical shift, of a few millielectronvolt (Shinohara 1961). The problem of explaining the observed chemical shift will be referred to as the 'Group III acceptor puzzle'.

4.3.1. *Group III acceptors as shallow centres—EMA with CCC*

The first satisfactory attempt to solve the puzzle is due to Lipari *et al.* (1980), who considered the correlation $\Delta E \propto (r-r_{Si})^2$ as a red herring and looked for a completely different explanation. First, Lipari *et al.* compared the ionization energies of Group III acceptors in silicon and germanium (as defined by Lipari *et al.*) and observed the same trend in silicon as in germanium (see table 12). Then they added to the Coulomb potential (5) (corrected to take into account the frequency dependence of the dielectric function) a strong short-range potential containing only one free parameter (α') which accounts for differences in the electronic structures of the ionic cores of various acceptors as well as in the lattice relaxation around them. Then, in view of the inherent difficulties in calculating α' from first principles, they selected the value of this parameter to reproduce the observed ground-state binding energies. Their results are in

Table 12. Ionization energies of acceptors in silicon and germanium.

	E_{ion}/meV	
Element	Silicon	Germanium
B	45·83	10·8
Al	70·42	11·14
Ga	74·16	11·30
In	156·94	11·99
Tl	247·67	13·43

table 13. Inspection of this table shows that for any given acceptor the value of α' in silicon is about the same as in germanium. This fact led Lipari *et al.* to conclude that 'the quasi-transferability of the short-range potentials from Si to Ge [...] clearly indicates that the short-range part of the impurity potential is more related to the atomic properties of the impurity than to the properties of the host lattice'. This seems to deny the possibility that the chemical shift is due to an elastic effect. However, in our opinion the calculations by Lipari *et al.* do not solve the Group III acceptor puzzle, but shift it to find the reason for the correlation between the strength of the short-range potential (through α') and $r - r_{Si}$.

Table 13. Best fit values of α'.

	α'/a_0^H	
Element	Silicon	Germanium
B	3·00	3·00
Al	1·01	1·10
Ga	0·93	0·93
In	0·73	0·70
Tl	0·63	0·57

In addition, the STSD seems unable to explain the following experimental evidence on chemical, equilibrium and transport properties of acceptors in silicon.

(1) Acceptors in silicon are deactivated by atomic hydrogen (Sah *et al.* 1983, 1984, Pankove *et al.* 1983, 1984, Gale *et al.* 1983, Hansen *et al.* 1984).
(2) An almost complete electrical activation at room temperature up to a concentration of some 10^{18} cm^{-3} (obtainable in metastable phase) is observed in Si : In (Cerofolini *et al.* 1983 a).
(3) The ionization energy of aluminium and gallium, determined with optical methods, E_{ion}, is a little different from the one determined with thermal methods, E_{th} (Milnes 1973). For indium, however, E_{ion} and E_{th} differ largely (Cerofolini *et al.* 1985 b). Table 14 shows these differences.
(4) 'Supershallow levels', i.e. levels with thermal ionization energy much lower than the one predicted by the EMA, are observed in neutron-irradiated Si : Ga (Fischer and Mitchel 1984, 1985) after annealing at moderate temperature (in the range 400–700°C), and in Si : In samples heated at temperatures so high, above 1100°C, to suggest they are not associated with process defects, but rather with the intrinsic dopant centre (Cerofolini *et al.* 1985 b).

Table 14. Ionization energies in silicon determined with optical and thermal methods.

Element	E_{ion}/meV	E_{th}/meV
B	44	45
Al	69	57
Ga	73	65
In	156	18
Tl	246	?

(5) A non-linear conductivity increase of several orders of magnitude is observed in illuminated Ge : Ga samples, even for frequency ν of incident radiation much lower than the ionization energy of gallium in germanium, $h\nu \approx 2{\cdot}5$ meV against $E_{ion} \approx 11$ meV (Leung and Drew 1984).

4.3.2. *Group III acceptors as deep centres*

The basic ideas to explain all the above evidence are the following (Cerofolini 1983, Cerofolini and Bez 1987).

(1) *Deep ground state.* In the ground state, the acceptor atom has a deep sp^2 hybridization, i.e. forms covalent bonds with three nearest-neighbour silicon atoms, the fourth atom remaining with a dangling bond,

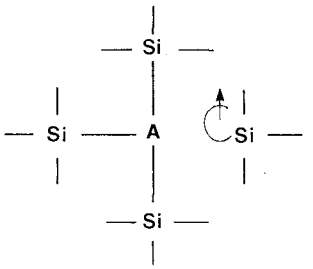

Even in the sp^2 state, a cloud of displaced silicon atoms surrounds the acceptor atom. This cloud is large enough to be considered as a small macro-system (SMS) embedded in the crystal. The crystal can be thought of as a heat reservoir while the SMS can be described in terms of thermodynamical quantities. The existence of large entropy effects for substitutional impurities in silicon and germanium due to the difference of tetrahedral radii was inferred by Cappelletti *et al.* (1982 b) from solid solubility data.

(2) *Shallow excited state.* Only when ionized, the acceptor has an sp^3 hybridization with a free hole in an excited state; this configuration is referred to as $sp^3 + h^+$. In this condition the acceptor atom has four covalent bonds with so many silicon atoms,

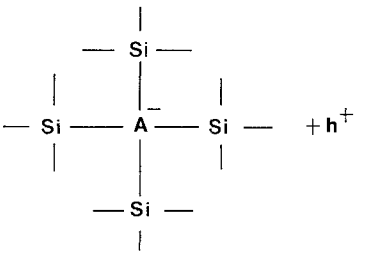

As a consequence of the difference between their respective tetrahedral radii, the acceptor–silicon covalent bond has a different length in comparison with the silicon–silicon covalent bond. This difference will produce a strain field in the crystal, described, for instance, by the elastic continuum theory as in Baldereschi and Hopfield (1972).

This model will be referred to as the deep dopant description (DDD) of acceptors. Because of assumptions 1 and 2, the transition from the sp^2 to the $(sp^3_- + h^+)$ configuration implies an elastic energy variation. Thus the chemical shift may be ascribed to the sum of two terms, $\Delta E = \Delta E_{el} + \delta$, ΔE_{el} being the elastic energy variation in the transition between the two configurations and δ the electronic energy variation. In turn, ΔE_{el} can be expressed by the relationship $\Delta E_{el} = \frac{1}{2}k[\kappa(r - r_{Si})]^2$, where k is the elastic constant of the $(sp^3_- + h^+)$ state and κ takes into account the fact that only a part of the difference $r - r_{Si}$ strains the lattice, while the other is absorbed by the bond. Baldereschi and Hopfield (1972) calculated κ for some isovalent impurities in silicon (Ge, Sn, Pb); in this case κ may be assumed constant, $\kappa \simeq 0{\cdot}4$, and we accept this value for all Group III impurities also.

The comparison of ΔE_{el} with ΔE is given in table 15 which suggests a negligible electronic contribution δ to the chemical shift, this quantity being almost equal to the elastic energy.

The DDD explains evidence (1)–(5) in Section 4.3.1 as follows:

Table 15. Comparison of the elastic energy with chemical shift.

Element	ΔE/eV	ΔE_{el}/eV
Al	0·012	0·013
Ga	0·016	0·013
In	0·099	0·119
Tl	0·189	0·148

(1) Boron inactivation by hydrogen has been demonstrated to lead to a final state where boron has a sp^2 hybridization and hydrogen saturates a silicon dangling bond:

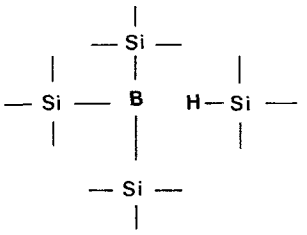

This model was demonstrated by Pankove *et al.* (1985 a) who also invalidated other proposed models for boron inactivation. The acceptor deactivation due to atomic hydrogen is explained in a natural way by the DDD. Indeed, the silicon dangling bond reacts readily with atomic hydrogen and once the dangling bond has been destroyed by reaction with hydrogen, the acceptor can

no longer ionize. This mechanism is similar to the one considered for the inactivation of surface states at the $Si–SiO_2$ interface after reaction with hydrogen.

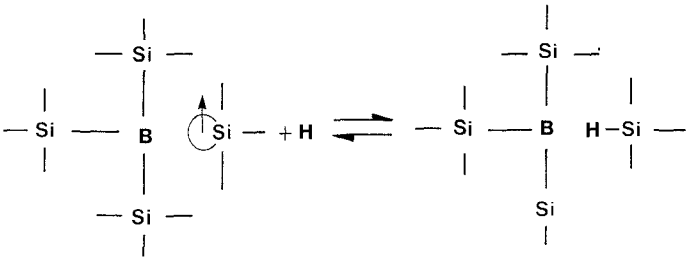

It is worth noting that the DDD assumes that inactivation may occur only for acceptors in the neutral state. Strong evidence that this is actually true was presented by Pankove *et al.* (1985 b) and by Johnson (1985).

(2) Indium is thermally activated with an energy of about 18 meV. The existence of this supershallow level for indium is spontaneously explained by the DDD considering the graph of figure 4 and invoking a central role of the SMS (Cerofolini and Bez 1987).

(3) In view of its low thermal ionization energy, at room temperature indium is almost completely ionized, even at high concentrations (up to $10^{18}\,cm^{-3}$).

(4) The evidence for the system Ge : Ge suggests extending the DDD of acceptors to germanium also. In fact, the behaviour of gallium in germanium is similar to that of indium in silicon.

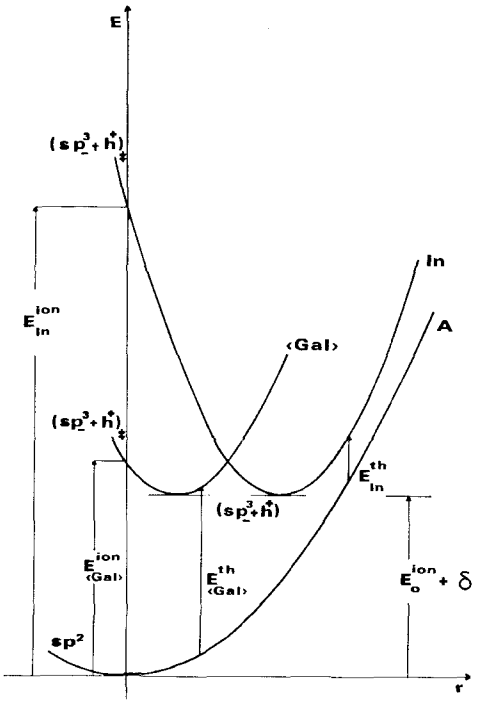

Figure 4. Configuration energy diagram for the ionization of acceptors in silicon. ‹Gal› denotes a hypothetical acceptor with properties intermediate between those of Ga and Al.

5. Defect–impurity interactions

Equilibrium defects and impurities, especially when present at high concentrations, can interact. Their interactions may in turn influence remarkably the behaviour of both defects and impurities. In principle we must consider three kinds of interactions: defect–defect interactions; impurity–impurity interactions; and defect–impurity interactions. In this section 'defect' will be the short form of 'equilibrium defect'.

The defect–defect interaction has two aspects: (1) interactions between point-like defects; and (2) interactions between surface and point-like defects. The interaction between point-like defects is responsible for the formation of: di-interstitials (i-i), di-vacancies (v-v), vacancy-interstitial pairs (v-i), large clusters, ESFs and ISFs. The stability of the v-i pair has been discussed in Section 2.3; for stress reasons, the i-i pair is supposed to be stable while the v-v pair seems unstable (Das 1983). The problem of the interaction between the surface and point-like defects is very complex. It is usually assumed that heat treatment in an inert atmosphere allows surface reconstruction so that at a silicon surface one can tentatively impose the equilibrium concentration of vacancies and self-interstitials. We do not share this opinion and believe that the above condition holds true only for unoxidized surfaces. With the exception of particular cases, e.g. surfaces obtained by cleavage in vacuum and kept in the same environment, it is also questionable whether or not free (hence reconstructable) surfaces exist.

The impurity–impurity interactions may concern atoms of the *same chemical species*, e.g. clusters or precipitates, or atoms of *different chemical species*, e.g. the X centres. Precipitation phenomena are usually relevant in the high-density limit only, and will not be considered here; we quote only that substitutional impurities of Groups III, IV and V have solid solubilities scarcely dependent on temperature, suggesting that this quantity is limited by entropic factors; the role of the tetrahedral radius on this factor is in evidence through the considerations of Cappelletti *et al.* (1982 b). The X centres are considered in Section 5.3 because they can throw light on the Group III acceptor puzzle. This section is mainly devoted to the study of defect–impurity interactions.

5.1. *Defect influence on impurities*

Knowledge of the influence of defects on impurities usually comes from the interpretation of diffusivity experiments. Because of the open structure of silicon crystal, *interstitial atoms* not covalently bonded to silicon, e.g. metals, diffuse from one site to another with relative ease, the diffusion coefficient being in the range 10^{-7}–10^{-5} cm^2/s at 1000°C. If covalent bonds are involved, e.g. interstitial oxygen, the diffusion coefficient is remarkably lower, of the order of 10^{-12} cm^2/s at 1000°C.

Substitutional atoms, namely Group III acceptors, Group V donors, carbon and germanium, on the contrary, are characterized by much lower diffusivities, below 10^{-14} cm^2/s at the same temperature.

About the diffusivity of *vacancies* and *self-interstitials* everything and its contrary, has been said: 'at room temperature... vacancies and interstitials are mobile in silicon' (Lannoo and Bourgouin 1981); 'the diffusivity of the vacancies is much higher than that of self-interstitials' (Zulehner and Huber 1982); 'once formed, vacancies are fairly immobile' (Das 1983). In addition, the most recent experimental results and theoretical calculations give opposite results: for instance, we have quoted the experimental results of Taniguchi *et al.* (1983) giving a low formation energy (0·7 eV) and high migration activation energy (4·0 eV), and the extended theoretical calculations by Car *et al.* (1984) giving a high formation energy (5–8 eV) and negligible migration barriers (0–0·5 eV).

In spite of this hazy situation, it is usually assumed that in the temperature range 800–1200°C the diffusivity at 1000°C being much higher than some 10^{-14} cm^2/s.

Various diffusion mechanisms of substitutional impurities have been proposed; the ones most frequently considered are: (1) *direct interchange* with neighbouring silicon atoms; (2) *cooperative interchange*, in which several cooperative moves occur simultaneously; (3) movement into an adjacent vacancy (*vacancy mechanism*); and (4) *interstitialcy*, in which the atom occupies an interstitial site and hence moves fast until it finds a vacant site. While modes (1) and (2) are usually assumed to occur only at very high temperatures because of the high energy involved in the process, modes (3) and (4) are usually assumed to occur for diffusion in the temperature range 800–1200°C.

5.1.1. *Vacancy mechanism*

The vacancy mechanism is based on the following hypotheses (Fair 1977): (1) the impurity, El, reacts with the vacancy to form an unstable pair; (2) impurity diffusion occurs by intercharge with an adjacent vacancy; (3) the concentrations of El-v pairs is proportional to $N_{El}N_v$; (4) the impurity diffuses only when in pair with a vacancy; (5) the vacancy concentration in the neutral state is the equilibrium one; (6) vacancies have different diffusivities in relation to their ionization state; and (7) the vacancy concentration in a given ionization state is determined by the Fermi energy.

Up to hypothesis (6) the diffusion process remains linear with impurity concentration N_{El}; when the impurity is a dopant, however, its concentration influences the Fermi energy so that non-linearities are introduced by assumption (7). The major phenomenological basis for such an assumption is that at a given temperature T non-linearities are usually observed when a dopant concentration N_{El} exceeds the intrinsic carrier concentration $n_i(T)$. The vacancy mechanism allows a mathematical modelling and is currently implemented in process simulation programs (Antoniadis and Dutton 1979).

5.1.2. *Interstitialcy*

The interstitialcy mechanism is based on the hypothesis that a substitutional atom, once injected in an interstitial position, has a high diffusivity. The conjecture of the interstitialcy mechanism comes from diffusion experiments in oxidizing environments. It has been positively demonstrated that diffusion during oxidation below 1200°C of some dopants, e.g. phosphorus and boron, occurs with higher diffusivity than in an inert atmosphere (Allen and Anand 1971, Masetti *et al.* 1973, 1976, Antoniadis *et al.* 1978, Taniguchi *et al.* 1980). This phenomenon is known as oxidation-enhanced diffusion. Since in the same temperature range oxidation injects self-interstitials (see Section 5.2.1), it is natural to guess that during oxidation the equilibrium

$$Si_i + El \rightleftharpoons Si + El_i \rightsquigarrow$$

is shifted toward the right hand side. The symbol $\rightsquigarrow$ (chosen in analogy with $\downarrow$ ('precipitates') and $\uparrow$ ('evaporates')) means 'diffuses away fast'.

Let us consider dopants which diffuse by the vacancy mechanism. They are characterized by oxidation-retarded diffusion, so that we can also infer that self-interstitials generated during oxidation partially recombine with vacancies. Other facts which suggest a strict correlation between oxidation-enhanced diffusion and interstitial excess are discussed by Fair (1981).

The mechanisms of dopant diffusion have long been matters of discussion and there are two major schools of thought: one school preferred the vacancy mechanism (Fair

1977) and the other the interstitialcy one (Seeger and Chik 1968). There is now general agreement that both mechanisms are effective in dopant diffusion, the relative weight of each mechanism being dependent on the nature of the dopant and diffusion temperature (Tan and Gösele 1985, Hu 1985).

5.2. *Impurity influence on defects*

The role of impurities on defects is usually studied by considering how impurities affect SFs—a decrease of ESF length is usually interpreted in terms of vacancy injection or interstitial absorption by impurities. No general relationship exists and in the following we shall consider a few examples which will be useful in other parts.

5.2.1. *Oxidation*

Oxidation at temperatures below 1200°C injects self-interstitials into silicon, this conclusion being based on the following experimental observations. In most experimental situations, ESFs which grow during oxidation have all the same length, which depends on the oxidation process (environment, temperature and time) (Murarka 1978). The constancy of ESF length is interpreted by assuming that ESF nucleation sites are at the surface, and the presence or absence of ESFs is ascribed to the presence or absence of ESF nuclei. In this case one speaks of an oxidation stacking fault (OSF). The OSF lies in a (111) plane, but rather than a disc it is a semi-ellipse with major axis at the surface, because self-interstitial excess is maximum just at the surface.

5.2.2. *Oxygen precipitation*

We have observed that oxygen precipitation puts silicon in a compressive state. If precipitates are large enough, the compressive energy is sufficient to form self-interstitials according to equation (4) and when they are in large excess with respect to their equilibrium concentration, can precipitate into ESFs. In an experimental study of oxygen precipitation kinetics in high-oxygen content silicon, Cerofolini and Polignano (1984) observed not only ESFs, but also structures lying in (111) planes, the etch pattern of which (after Secco etching) is the 'complementary' of the etch pattern of the ESF (see figure 5) and which was attributed to ISF. After isotropic $HNO_3 : CH_3\text{-}COOH : HF$ 5 : 3 : 1 etching to a depth of about 50 μm, it is possible to get a (100) plane crossing presumed ESFs and ISFs. The planar view of the etch pattern of these defects after Secco etching is shown in figure 6; again the etch pattern of the presumed ISF is the complementary of the ESF. The complete etch pattern can be interpreted by admitting the simultaneous presence of ESFs and ISFs, in agreement with the evidence for ISFs during oxygen precipitation by Claeys *et al.* (1984). In turn, the origin of ISFs can be explained only admitting a vacancy excess induced by precipitation. This process is possible (and mandatory) if stress is relieved in bulk silicon by injection of vacancy-interstitial pairs, rather than at the Si–SiO_2 (precipitate) interface by injection of self-interstitials.

5.2.3. *Indium precipitation*

Consider an impurity, the segregation coefficient of which between silicon and SiO_2 favours accumulation into silicon. If: (1) the oxidation rate is high compared to the diffusion rate; and (2) the equilibrium segregation is established at the Si–SiO_2 interface, then oxidation piles up the dopant in silicon close to the moving interface. This 'snow-plough' effect can increase the impurity concentration to values in excess of the solid solubility.

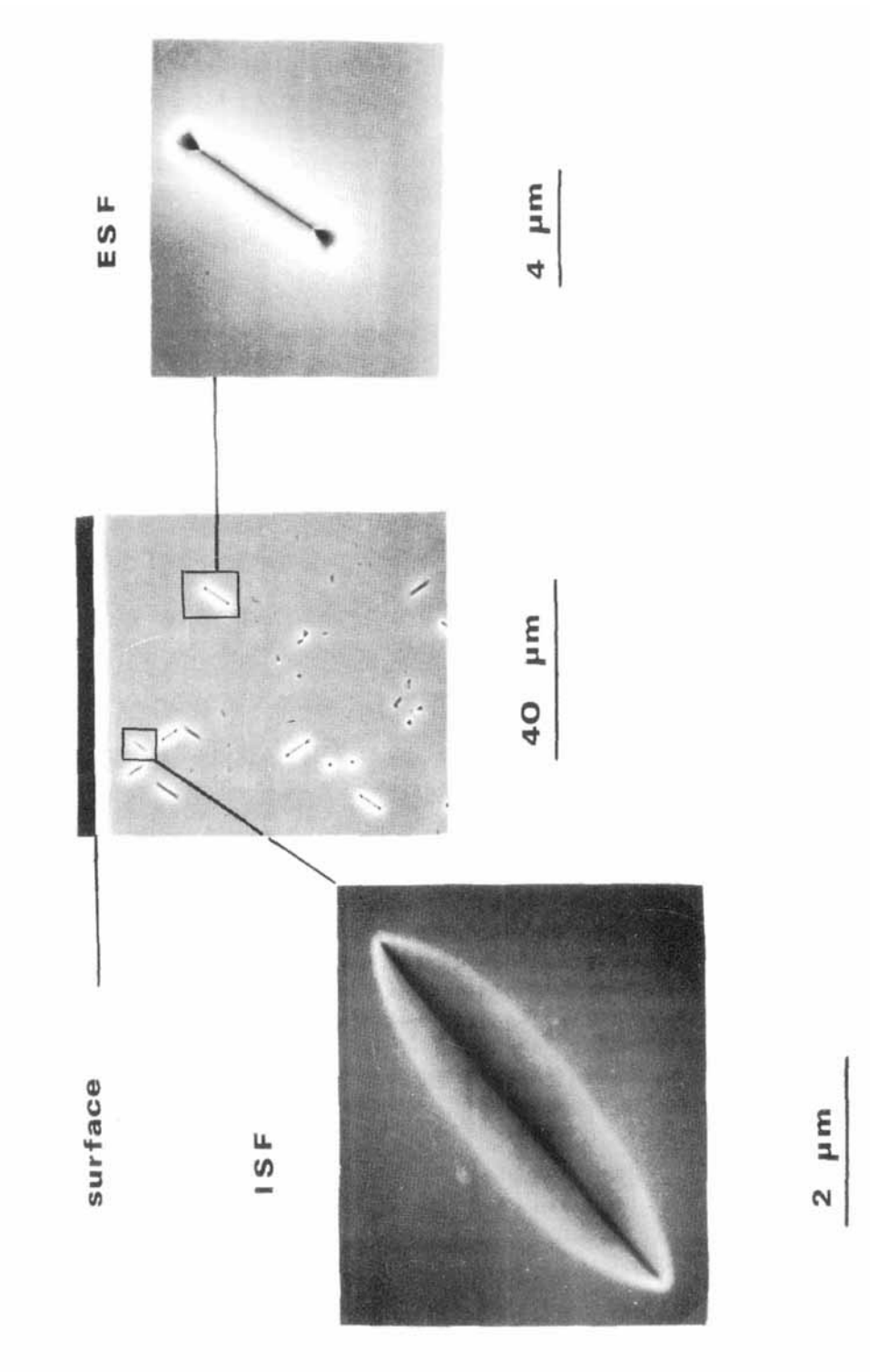

Figure 5. SEM view after Secco etching of a cleavage (111) plane after a heat treatment responsible for oxygen precipitation.

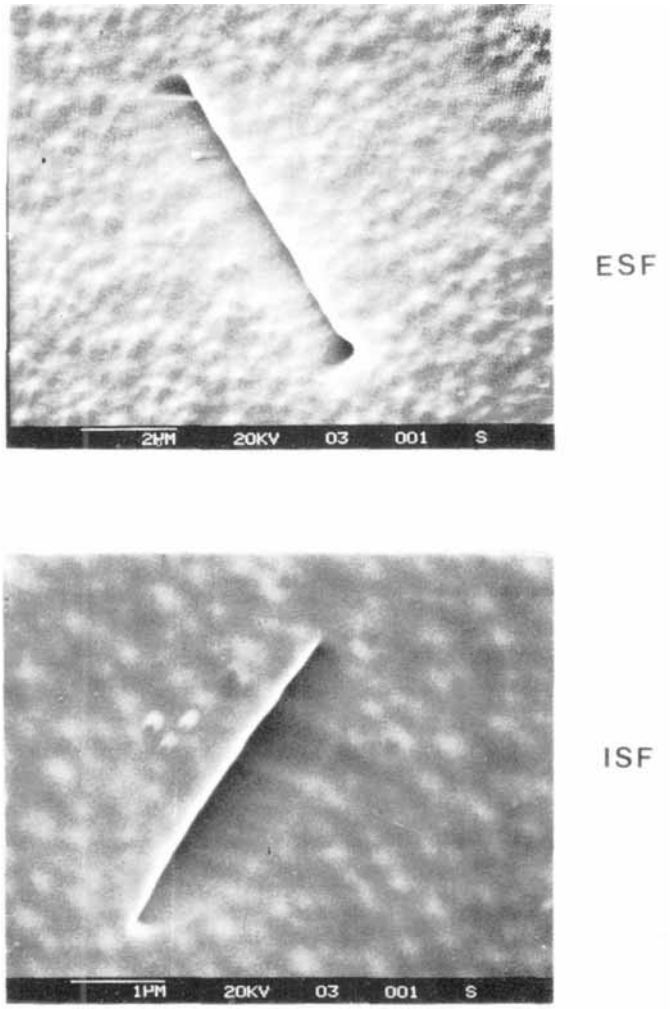

Figure 6. SEM view after isotropic and Secco etching of bulk defects crossing the (100) surface.

For indium, pile-up at the Si-SiO_2 interface during oxidation has been observed by Rutherford back scattering (Cerofolini *et al.* 1983 b, c). In that work it was also shown that:

(1) samples with pre-existing precipitates showed ESFs of variable length after oxidation and Secco etching, thus showing that precipitation (which is more effective at the surface, but extends also in depth) produces self-interstitial excess and SF nuclei; and

(2) samples without precipitates showed, after oxidation and Secco etching, a bimodal distribution of ESF length. Long ESFs have all the same length, thus suggesting that they are OSF starting from SF nuclei at the surface; short ESFs, again of the same length, indicate that at a certain stage during oxidation there is a sudden injection of self-interstitials, probably due to indium precipitation after pile-up.

5.3. *An example of impurity–impurity interaction—the X centre*

An acceptor level involving indium, called the X centre, was observed in Hall experiments and optical absorption data by Baron *et al.* (1977) and Scott (1978), respectively. Baron *et al.* (1979) postulated that the X centre is an In-C complex, and Jones *et al.* (1981) have shown that each acceptor has its own X centre, i.e. each acceptor forms a relatively stable complex with carbon to give an acceptor level. Table 16, taken from Jones *et al.*, compares the ionization energies of all Group III acceptors along with those of their own X centres.

The reason for the relative stability of the acceptor-carbon A–C complex is probably that the pure ionized acceptor (except boron) is subjected to a compressive stress (see table 11); this stress is diminished if the acceptor is bonded to an atom with a tetrahedral radius smaller than r_{Si} ($r_C = 0{\cdot}77$ Å, whereas $r_{Si} = 1{\cdot}17$ Å). Through the formation of an X centre there is the possibility of a local stress relief.

For the X centre, too, there is the problem of explaining its chemical shift. Calculations by Searle *et al.* (1982, 1983) show that the chemical shifts of X centres can be explained by a CCC-EMA. However, the DDD of acceptors is also able to explain it in a natural fashion. In this model the chemical shift of the X centre, ΔE_{AC}, is a fraction of the chemical shift of the corresponding acceptor ΔE_A. This fraction is probably negligible for acceptors (Al or Ga) which involve small lattice deformation. This is because the impurity can maintain the tetrahedral hybridization without lattice deformation via a modest shift towards the adjacent C atom, and must be close to $\frac{3}{4}$ for acceptors with a large tetrahedral radius (In, Tl), since in this case the sp^2 hybridization necessarily involves the compression of three bonds, while the fourth bond has the possibility of relaxing.

Table 17 (Cerofolini 1983) compares the chemical shifts of acceptors with those of their X centres and with the values predicted by the DDD.

Table 16. Optical ionization energies of acceptors and their X centres.

	E_{ion}/eV	
Element	Pure	X centre
B	0·044	0·037
Al	0·069	0·056
Ga	0·073	0·057
In	0·156	0·113
Tl	0·246	0·180

Table 17. Chemical shifts of acceptors and their X centres.

Element	ΔE_A/eV	ΔE_{AC}/eV	ΔE_{AC}/eV (expected)
Al	0·012	−0·001	≃0
Ga	0·016	0·000	≃0
In	0·099	0·056	≃0·07
Tl	0·189	0·123	≃0·14

6. Surfaces and interfaces

Several phenomena involve surfaces, some of them concerning only crystal atoms and others impurities. Intrinsic phenomena are: surface *relaxation*, i.e. the displacement of planes close to the surface from their lattice position, and *reconstruction*, i.e. the formation of a specific surface structure with symmetry different from that of the crystal. Extrinsic phenomena are: *segregation* of impurities at, or far from, the surface; *formation of surface compounds*, this process possibly being the final result of segregation at the surface; *chemisorption* from gases or liquids, terminating at the first layer or proceeding up to the formation of multilayered structures. *Oxidation* is an important example of the last process.

The major technological interest, rather than being on the silicon surface, is on the $Si–SiO_2$ interface, because of its very low defect density. The $Si–SiO_2$ interface is characterized by *proper* and *improper* defects. Proper defects are inherently associated with the oxidation process or subsequent heat treatments; improper defects are all other defects, such as the ones due to alkali ion contamination or to radiation damage.

This section deals only with proper defects, though they are relevant only when all other defects have been reduced to a negligible amount. For instance, Na^+ contamination is responsible for a positive charge in the oxide, this charge being mobile under the action of an electric field. This mobile charge gives rise to uncontrollable shifts in threshold voltage of metal-oxide-semiconductor (MOS) transistors such that their practical use was impossible for many years. Only the use of very accurate cleaning procedures (washing with de-ionized water, with resistivity higher than $5\,M\Omega\,cm$), oxidation in the presence of HCl (to form volatile alkali chlorides), and gettering by $SiO_2:P_2O_5$ (redistribution between SiO_2 and $SiO_2:P_2O_5$ favours Na^+ accumulation in the doped oxide) allow the Na^+ mobile charge to be reduced to a negligible amount.

A silicon atom in bulk silicon is bonded to four silicon atoms. Let us define the 'oxygen coordination number' of a given silicon atom as the number of oxygen atoms to which it is bonded. The region where the oxygen coordination number differs from 0 or 4 is referred to as the *interface region*. Representations of compounds with oxygen coordination number equal to 1, 2 or 3 are:

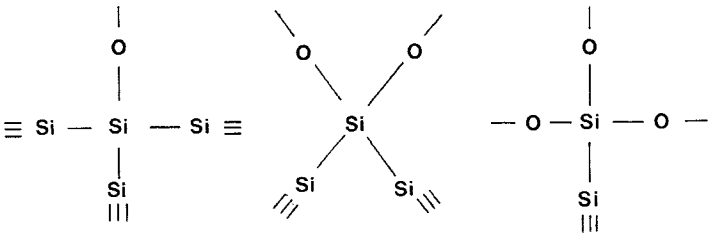

The width of the interface region has been extensively investigated; in particular: Johannessen *et al.* (1976) found an upper limit of 35 Å to the interface region; Helms *et al.* (1978) lowered this limit to 20 Å; and Helms *et al.* (1979) found that this width is independent of oxide thickness x_{ox}, at least in the interval $400\,Å \leqslant x_{ox} \leqslant 1000\,Å$. The intrinsic defects are contained in the interface region.

6.1. *Interface defects*

The proper interface defects are classified as *fixed charge*, if they cannot exchange electrons or holes with the lattice, and *interface traps* if their charge sfate can be modified by varying the Fermi energy E_F.

For the amount per unit area of fixed charge and interface traps we use the symbols N_f and N_{it}, respectively, suggested by the Electrochemical Society—IEEE Committee (Deal 1980).

6.1.1. *Fixed charge*

The fixed charge is a positive charge confined within 20 Å from the Si–SiO_2 interface. The amount of fixed charge is usually determined by measuring the shift of flat-band voltage in high-frequency capacitance-voltage ($C-V$) characteristics of MOS capacitors (Goetzberger *et al.* 1976). The fixed charge depends on both oxidation-anneal and surface properties. The dependence on oxidation-anneal conditions is summarized in the Deal (1974) triangle (see figure 7). Starting from an oxidized surface with low N_f ($N_f \approx 10^{10}\,cm^{-2}$), further oxidation at low temperatures ($T \approx 600°C$) is responsible for an increase of fixed charge by some orders of magnitude (typically to $10^{12}\,cm^{-2}$). Heat treatments at about 1200°C, both in an inert or oxidizing atmosphere, reduce N_f to values as low as $10^{10}\,cm^{-2}$. Further annealing in an inert atmosphere at lower temperature does not yield further increase of N_f.

This behaviour suggests that, in order to obtain a thin oxide with a low fixed charge density, the oxidation cycle must be carried out as follows: oxidation at low T, to control accurately oxide thickness; anneal at high T in an inert atmosphere to reduce N_f; and extraction at low T in an inert atmosphere.

The dependence of N_f on the surface structure is contained in the following observation: irrespective of the oxidation-anneal conditions, $N_f(111)/N_f(100) \approx 3$, i.e. this ratio is roughly equal to the ratio of surface atomic densities of the (111) plane to the (100) plane—the higher the surface density, the higher the fixed charge.

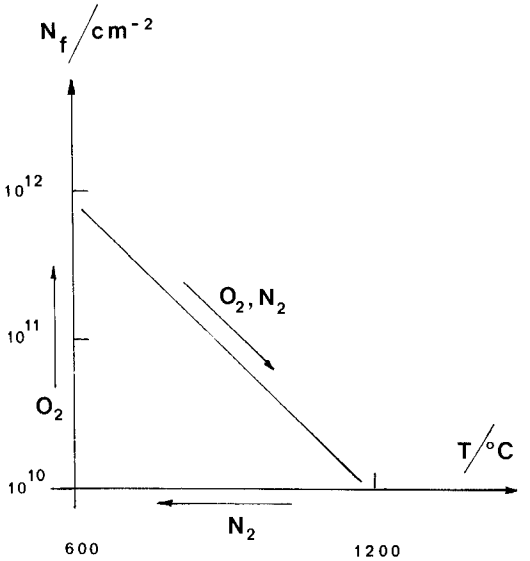

Figure 7. Deal triangle.

6.1.2. *Interface traps*

Interface traps can exchange electrons or holes with the lattice. Since the interface states are characterized by a low velocity of trapping–detrapping, they can be observed by studying the quasi-static $C-V$ characteristics of MOS capacitors (Berglund 1966). These characteristics can be handled to obtain a quantity $g_{it}^{\circ}(E_F)$ related to the actual interface trap density in the gap $g_{it}(E)$ through the relationship (Cerofolini *et al.* 1980)

$$g_{it}^{\circ}(E_F) = \int_{E_V}^{E_C} F_T(E_F, E) g_{it}(E)\, dE \tag{14}$$

where $F_T(E_F, E)$ is a function related to the Fermi–Dirac distribution.

For well-prepared surfaces, the function $g_{it}^{\circ}(E)$ has two maxima at about 100 meV from the conduction and valence band edges, and one minimum roughly at midgap. The problem of solving eqn. (14) for $g_{it}(E)$ is improperly posed, and the particular form of $g_{it}^{\circ}(E_F)$ (with the maxima at the extremities of the admissible physical range) forbids even an approximate estimation of $g_{it}(E)$. The experimental $g_{it}^{\circ}(E)$ is, however, compatible with two somewhat broadened Dirac delta distributions at about 100 meV from the bottom of the conduction band and the top of the valence band, respectively.

The interface traps are generated simultaneously with the fixed charge. In fact, immediately after oxidation and irrespective of the oxidation conditions (leading to high or low N_f), one has

$$N_f \approx N_{it} \tag{15}$$

However, interface traps can be destroyed independently of fixed charge by heat treatments at about 450°C in a hydrogen atmosphere; heat treatments at higher temperatures (>500°C) regenerate the interface traps.

6.2. *Structure*

Because of the weak equality (15), one could be tempted to explain the nature of interface traps in terms of bound states in the coulombic field of the positive fixed charge. Such an explanation, however, suffers from two difficulties: it does not account for the bound state of holes and for the anneal behaviour in hydrogen which causes drastic deviations from the weak equality (15).

A model for the fixed charge and interface trap must explain: (*a*) the localization of these defects at the interface; (*b*) how they are generated simultaneously; (*c*) the amphoteric nature of interface traps; and (*d*) why only interface traps and not fixed charges interact with hydrogen. A model which explains these four characteristics is the following, essentially due to Raider and Berman (1978).

Interface trap and fixed charges are formed simultaneously during oxidation by reaction of oxygen with an interface Si–Si bond

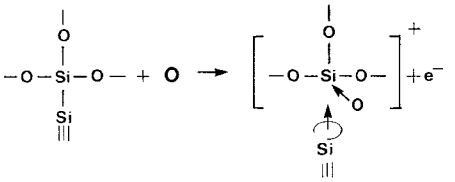

(A)

The positive Si–O complex

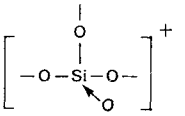

is the positive fixed charge, while the site

is the interface trap.

The positive Si–O complex is assumed to be stable at low temperature ($<800°C$), but destroyed at high temperature ($>1000°C$) by the following mechanism:

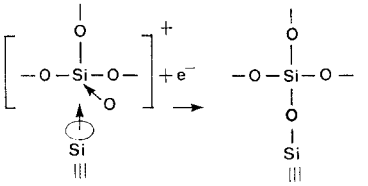

(B)

which simultaneously destroys the interface trap.

The above model explains in a natural way the features from (*a*) to (*d*). In fact:

both intrinsic defects are at the interface;
the positive charge and interface trap are simultaneously formed (reaction A) and destroyed (reaction B);
the interface trap has an amphoteric character

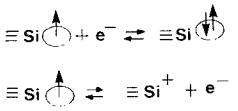

while the fixed charge cannot react with hydrogen, the silicon dangling bond can readily be destroyed by interaction with hydrogen

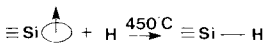

once saturated with hydrogen, the bond cannot further exchange electrons with the lattice;
heat treatments at $T>500°C$ destroy the Si–H bond, as it is well known from silane chemistry; and
the Deal triangle is explained by the assumed stability range of the positive Si–O complex.

6.3. *Electronic structure of interface defects*

Because of these assumed structures, the interface traps could be active in electron-spin resonance (ESR). A detailed ESR analysis of interface defects was carried out by Caplan *et al.* (1979) and Poindexter *et al.* (1981). These authors observed two intrinsic ESR signals, named P_a and P_b. The P_a signal has an isotropic character, and resembles the signal from conduction electrons.

On (111) wafers the P_b signal, first identified by Nishi (1966, 1971), is found to be located at the Si–SiO_2 interface; its anisotropy is similar to that of bulk silicon defects having silicon bonded to three other silicon atoms and is in no way related to the E′ centre in SiO_2 (oxygen vacancy). In addition, both the P_b signal and N_{it} were found to be greatly reduced by steam oxidation and hydrogen annealing, while both are regenerated by subsequent annealing in a nitrogen atmosphere. These facts allow us to identify P_b with N_{it} and give a clear indication that N_{it} is therefore formed by unpaired electrons as previously sketched. The situation is less clear for (100) wafers.

The N_f centre, as shown in the previous sections, is not ESR active because it is positively charged and does not contain unpaired electrons. The absence of the E′ signal, associated with an oxygen vacancy in SiO_2, is therefore not contradictory with the assumed fixed-charge structure.

6.4. *Influence of interface defects on oxidation kinetics*

Silicon oxidation kinetics in different (dry oxygen and steam) environments have been studied extensively. Dry oxidation is relatively slow, while steam oxidation is much faster. For fast (steam) oxidations, the kinetics are well described by the linear-parabolic law

$$\frac{x_{ox}^2}{k_p}+\frac{x_{ox}}{k_l}=(t+t_0) \tag{16}$$

due to Deal and Grove (1965). This law relates the SiO_2 thickness, x_{ox}, to the oxidation time t and contains three parameters: the kinetic coefficients k_p and k_l and the characteristic time t_0. The kinetic parameters define two oxidation ranges: the linear regime, where the oxide thickness grows linearly with oxidation time t

$$x_{ox}\ll k_p/k_l \Rightarrow x_{ox}\simeq k_l(t+t_0); \tag{17}$$

and the parabolic regime, where the oxide thickness grows parabolically with oxidation time

$$x_{ox}\gg k_p/k_l \Rightarrow x_{ox}\simeq (k_p(t+t_0))^{1/2}. \tag{18}$$

Kinetics (17) are due to the fact that the rate-limiting step is oxidation of interface silicon atoms, while kinetics (18) hold true when the rate limiting step is oxygen or hydroxyl diffusion through the oxide.

The characteristic time t_0 is related to the oxide thickness x_{ox}^0 at time $t=0$:

$$t_0=x_{ox}^0/k_l+(x_{ox}^0)^2/k_p$$

and for freshly prepared surfaces under high vacuum $t_0=0$.

In practice, the characteristic time t_0 is often obtained by extrapolation of actual linear kinetics (17) for $t\to 0$, that gives also $x_{ox}^0\approx 20$–40 Å, and this thickness is usually interpreted as the thickness of the 'native oxide'. This interpretation, however, is false. The falsity of such an opinion is demonstrated, for instance, by neutron activation analysis and X-ray photoelectron spectroscopy (Mende *et al.* 1983) showing that the oxide grown on freshly prepared silicon after exposure to air at room temperature and pressure is less than one monolayer. These studies also showed that room-temperature oxidation of silicon occurs in agreement with the Elovich isotherm, $x_{ox}-x_{ox}^0\propto \ln t$. The discrepancy between the common opinion about the native oxide and the above results can be removed by admitting that equation (17) does not hold true in the first stages of oxidation.

The first attempt in such a direction was contributed by Hu (1983, 1984) who replaced the Henry adsorption isotherm (responsible for the linear kinetics (17)) by the Freundlich isotherm. After such a replacement, one arrives at an equation which behaves as equation (16) for a long period, but which deviates in the early stages.

6.5. *Surface reconstructibility*

This section is devoted to the study of self-reconstruction phenomena and their influence on intrinsic defects.

It is usually accepted that a surface under *oxidation conditions* at $T < 1200°C$ injects self-interstitials into silicon. In the hypotheses listed at the end of the previous section, under these conditions a surface continuously reconstructs leaving an equilibrium distribution of oxygen adsorption sites. Self-interstitial injection must necessarily be invoked to explain OSF growth and OED.

The *nitridation process*, $3Si + 4NH_3 \rightarrow Si_3N_4 + 6H_2$, injects vacancies into silicon and in this light it can be seen as the counterpart of oxidation (Fahey *et al.* 1983, 1985). A detailed study of diffusion under oxidation–nitridation can be found in Fahey (1985).

For heat treatments in an *inert atmosphere*, we can distinguish two cases as follows. For a *free surface*, obtained, for instance, by cleavage in high vacuum and kept therein, we can hypothesize that surface reconstruction is possible (tending toward a more stable surface structure) and vacancies and self-interstitials can be injected/absorbed independently of one another, eventually reaching a concentration close to the equilibrium one in a layer of width of the order of their diffusion length. In this case, the surface can be seen as a boundary with infinite v-i generation-recombination rate and v-i profiles can be calculated by solving the Fick equation under the following boundary-initial conditions:

$$C_i(0, t) = C_i^{eq}, \qquad C_v(0, t) = C_v^{eq}$$

and

$$C_i(x, 0) = \bar{C}_i, \qquad C_v(x, 0) = \bar{C}_v$$

where $\bar{C}$ denotes a given concentration, e.g. the equilibrium concentration at the temperature T at which the sample was quenched. For *constrained surfaces*, we can limit outselves to the $Si–SiO_2$ or $Si–Si_3N_4$ ones because at the moment they are of practical interest.

In these cases the only way for vacancies and self-interstitials to reach equilibrium independently is to destroy interface bonds and eventually to reconstruct them. But this process is rather slow because of the strength of these bonds, so it is not unreasonable to admit that in these cases vacancies and self-interstitials are generated in pairs in bulk silicon with the mechanism considered in Section 2.3.

7. Gettering

Silicon single crystals for semiconductor device applications are usually produced in the form of slices, with diameter in the range 5–15 cm and thickness in the range 0·02–0·06 cm. The slice is then characterized by two major surfaces—the *front* and *back*. These surfaces have very different mechanical finishing: the front is mirror finished with extremely low roughness (peak-to-peak average distance of about 30 Å), while the back is usually strongly damaged for reasons which will become clear in the following subsections.

By 'extended defect' we mean a macroscopic portion of silicon where the crystal symmetry is lost. The dimensionality, D, of an extended defect can be lower than 3.

Extended defects may involve only silicon atoms (e.g. SFs ($D=2$) and dislocations ($D=1$)), impurities (e.g. precipitates ($D=3$)) or silicon-impurity complexes, e.g. the swirl defect.

Though a clear correlation between extended defects and electrical defects has not yet been established (however, SFs seem to reduce lifetime in capacitors (Strack *et al.* 1979) and to increase leakage current in diodes (Murarka *et al.* 1979)), in semiconductor processing one usually assumes the validity of the *aesthetic principle*: beautiful = good, where 'beautiful' means 'free of extended defects' and 'good' means 'free of electrical defects'. In this light, all care is taken to avoid the growth of extended defects during processing. Though the starting material is usually provided free of dislocations and SFs, a typical device process cannot maintain this limit. It suffices, however, that this limit is maintained in a limited portion of silicon, i.e. in active zones, the extension of which depends upon the kind of device considered. For instance, in MOS devices, the layer of thickness around 10 μm from the front of the slice can be considered as the active zone. Two major techniques have been developed to fulfil the aesthetic principle—*external gettering* and *internal gettering*. These techniques are based upon very different principles, though they can be used in combination. The efficiency of a gettering technique is strongly linked with the whole process, and a high degree of empiricism is usually necessary to set up an efficient gettering technique; in the following we attempt its rationalization.

7.1. *External gettering*

7.1.1. *Dislocations*

First, we limit attention to dislocations. A typical device process involves: heat treatments in inert atmospheres, oxidations, deposition of layers, implantations and definitions of geometries. Because of the different expansion coefficients of the oxide or other layers with respect to silicon during a heat treatment, a stress arises. This stress may be very high, of the order of 10^9 dyn/cm^2, and may be responsible for plastic deformations.

The elastic limits at different temperatures for FZ and CZ silicon materials are given in figure 2 (Kondo 1981). Since the elastic limit decreases with temperature, it follows that the higher the temperature, the greater the possibility that the elastic stress is absorbed by silicon plastically, i.e. by forming dislocations. Hence, the first rule to avoid the formation of dislocations:

Rule 1: Heat treatments must be as mild as possible.

The comparison of the CZ plastic limit vs FZ gives the second rule to avoid the formation of dislocations:

Rule 2: As far as possible CZ materials are preferred to FZ.

These conditions alone, however, are not sufficient and other precautions must be taken. External gettering (EG) is based upon the following thermodynamic conjecture: *when both small and large defects are simultaneously present, heat treatments tend to enlarge large defects and to reduce (and eventually to annihilate) small defects.* This conjecture gives the following rule:

Rule 3: The backside must be rich in extended defects.

This condition can be satisfied starting either from a back already containing extended defects (obtained, for instance, by a local melting by laser irradiation, or by poly-silicon

deposition) or from a heavily damaged back (obtained by mechanical or chemical processes) which develops extended defects immediately after the first heat treatment. Examples of heavy back damage are the stresses produced by: mechanical working (sand blasting, brushing, and so on), phosphorus predeposition (because of the difference of tetrahedral radii between P and Si), and by Si_3N_4 deposition on the back (Rozgonyi *et al.* 1975, Petroff *et al.* 1975).

7.1.2. *Stacking faults*

The first and third rules should also avoid the growth of SFs. In fact, in order to organize themselves as ESFs, self-interstitials require the existence of nuclei at the surface. If the thermodynamic conjecture and rule 3 are satisfied, these nuclei tend to disappear, being gettered by extended defects at the back.

In addition, even admitting that the gettering process of SF nuclei is not completely effective, rule 1 ensures that the length of OSFs which are formed during the growth of an oxide of given thickness is small, so that they can be dissolved with relative ease by further annealing. This conclusion is reached considering the results by Murarka (1978), who showed that for a given thickness of grown SiO_2, the lengths of OSFs are an increasing function of the oxidation temperature (see table 18).

An additional procedure not to have formation of SFs consists in carrying out oxidations, responsible for i-injection and hence suspected for SF formation, in an atmosphere of HCl. Indeed, the following pathway seems to occur (Shimura and Craven 1984): Transition-metal impurities tend to segregate at the surface where precipitates may form; precipitates, in turn, are SF nuclei and once SFs are formed they are decorated by metals. Decorated SFs are eventually responsible for electrical failures. This vicious circle can be broken by carrying out the oxidation in HCl, because HCl reacts with metals to form volatile chlorides and so etches the SF nuclei.

Table 18. Length of OSFs grown during a dry oxidation to produce a layer of 1000 Å.

Temperature/°C	OSF length/μm
1050	3
1100	8
1150	15
1200	22

7.2. *Internal gettering*

We have already observed that in CZ materials the oxygen concentration exceeds the solid solubility, even at 1200°C. If heat treatments are carried out at temperatures high enough to allow oxygen diffusion but low enough that the oxygen concentration is higher than the over-saturation concentration, then precipitation actually occurs. At temperatures around 1000°C these conditions are satisfied in most cases. Since important device process steps are characterized by temperature close to 1000°C, care must be taken to prevent oxygen precipitation in active zones. This is attained if the oxygen concentration is lowered below the over-saturation concentration; this situation can be obtained by a suitable high-temperature evaporation from a region of depth comparable with the oxygen diffusion length. Such a process may also be responsible for oxygen precipitation in the bulk. This precipitation is beneficial because large oxygen precipitates in the bulk tend to dissolve small precipitates (embryos) in

active regions. In principle this high-temperature process leads to the formation of a zone free of both oxygen and oxygen precipitates close to the surface (the denuded zone, DZ) and of a strongly defective zone in the bulk (Tan *et al.* 1977).

Actually the detailed procedure to obtain a high-quality DZ depends upon oxygen content and the thermal history of the silicon (presence of pre-existing precipitates, other defects and so on), and two major variants to obtain it are known: the HI-LO-HI process, suitable for high oxygen concentration wafers, and the LO-HI process, suitable for low oxygen concentration wafers.

7.2.1. *High oxygen content, HI-LO-HI process*

For high oxygen content, ($8–10 \times 10^{17}\,cm^{-3}$), it is mandatory to avoid oxygen precipitation in the surface layer in the early stages. The first heat treatment (HI), therefore, must be done at high temperature (say $>1050°C$) to allow fast oxygen evaporation, and so it is possible that no precipitation occurs in the bulk. To activate the precipitation process, a heat treatment (LO) at low temperature (say around 750°C) is carried out and is responsible for the formation of nuclei. Subsequent annealing at high temperature (HI) is responsible for the growth of precipitates (Nagasawa *et al.* 1980).

In practice the second HI is represented by the whole device processing, and during the first HI process precipitation can take place by homogeneous nucleation too (while during the second HI, precipitation takes place by heterogeneous nucleation on pre-existing precipitates).

The effectiveness of the first HI is increased if the process is carried out in an oxidizing environment. Indeed, oxidation injects self-interstitials into silicon so that the oxidation-induced self-interstitial excess hampers oxygen precipitation because of the mass-action law applied to equation (4). This inhibition is effective to a depth of the order of the self-interstitial diffusion length.

7.2.2. *Low oxygen content, LO-HI process*

If the oxygen content is low ($5–8 \times 10^{17}\,cm^{-3}$), the following process is suitable for DZ formation. The first step, LO, is responsible for the formation of nuclei everywhere in the crystal. The second step, HI, is responsible for the heterogeneous nucleation of precipitates in the bulk and for nuclei dissolution close to the surface because the decreasing oxygen concentration makes them unstable (Yamamoto *et al.* 1980).

7.3. *Heavy-metal gettering*

By heavy metal we mean here any metal with filled d-orbitals. Once embedded into the silicon, because of their rich electronic structure, heavy metals can exchange electrons with conduction and valence bands, i.e. they can behave as generation-recombination centres. In most cases this is an unwanted characteristic and when heavy metals are present at concentrations higher than, say, $10^{15}\,cm^{-3}$, may be responsible for ill-functioning. Furthermore, heavy metals are fast diffusing and tend to segregate at the surface where they may precipitate because of their low solubility. In turn, metal precipitates are ESF nuclei as described in Section 7.1.2. Various techniques, often without a theoretical basis, have been proposed to control heavy metals; in our opinion we can distinguish two lines of thought.

7.3.1. *Early gettering*

Metal precipitates in active zones are responsible for electrical characteristics largely deviating from theoretical ones (Busta and Waggener 1977 a, b); in particular, precipitates in p-n junctions are responsible for soft behaviours. Precipitates were typical of the silicon prepared in the 1950s and 1960s, because of the high metal content in silicon ingots of those years. The major effort was then of forbidding metal precipitation. Precipitation at surfaces can be avoided by: increasing the solid solubility of metals; and making the segregation coefficient between surface and bulk as close as possible to 1. Both these goals can be accomplished if the temperature is kept high and the solid solubility is increased by heavy doping (Meek and Seidel 1975). This procedure was identified in a classic paper by Goetzberger and Shockley (1960) who proposed high-temperature heat treatments associated with heavy phosphorus predepositions as a gettering technique.

7.3.2. *Segregation gettering*

The continuously decreasing impurity content of commercial single-crystal silicon and the cleanliness of processes have practically ruled out the problem of metal precipitation. Heavy metals, however, are often dangerous even in solid solution because, being generation-recombination centres, they behave as lifetime killers. Hence the need for a technique able to remove heavy metals from the active zone. One such technique was suggested by Baldi *et al.* (1978 a, b) for gold gettering and, when used in semiconductor device processing (Baldi *et al.* 1980), led to the realization of ideal p-n junctions (Cerofolini and Ferla 1981, Cerofolini and Polignano 1984, Cappelletti *et al.* 1985).

The model of gettering by segregation annealing was presented in the communication *The getter devil and the theory of gettering* at the Los Angeles Symposium on Gettering in Semiconductors (Cerofolini and Ferla 1979): 'The getter devil is a dwarf who, inserted into a silicon matrix enjoys identifying and retaining heavy metal impurities walking in his neighbourhood. Just as his illustrious ancestor, the Maxwell demon, he can succeed in his hobby only if the capture is a spontaneous process and if impurities can actually reach his neighbourhood. "Spontaneous" means that if capture takes place at constant temperature and volume, the process is characterized by a negative free energy difference ΔF°_{*} of a gettered impurity with respect to a free impurity in the silicon matrix. In this case, the spontaneous process actually occurs if the getter devil is indeed visited by the metal atoms, i.e. if the temperature is high enough.

These considerations can be formalized as follows: Let the getter devil be formed by a family of n_* suitable getter sites at an atomic concentration N_*; at any given temperature in equilibrium conditions there is a preferential segregation described by the segregation coefficient

$$K = 1 + (N_*/N_{Si}) \exp(-\Delta F^{\circ}_{*}/k_B T) \tag{19}$$

where N_{Si} is the silicon atomic concentration, k_B is the Boltzmann constant and T the segregation temperature. Relationship (19) shows that K is higher the lower is T and the higher is N_*; these are the first two rules of gettering. The third rule is obtained by imposing that the total number of getter sites be greatly in excess of the total number of impurities, n_{imp}:

$$n_* \gg n_{imp} \tag{20}$$

A large K and the fulfilment of condition (20) are in themselves insufficient for gettering. Indeed, actually to reach equilibrium, we must heat the crystal to render metal impurities mobile along the matrix. From the physical point-of-view we can formalize this requirement by imposing that the volume v, described by a metal impurity during the duration t of the heat treatment, contains much more than one getter site:

$$vN_* \gg 1 \tag{21}$$

The theory of rate processes allows v to be estimated,

$$v = \varsigma b \nu_0 \exp(-E_m/k_B T)t \tag{22}$$

where ς is the cross section of a moving impurity ($\varsigma \approx 10^{-15}\,\mathrm{cm}^{-2}$), b is of the order of the silicon–silicon distance ($b \approx 2{\cdot}3$ Å), ν_0 is the vibration frequency of the metal atom in the ground state ($\nu_0 \approx 10^{13}\,\mathrm{s}^{-1}$) and E_m the activation energy for migration. Some values of E_m are given in the following: Ag, $E_m = 1{\cdot}60$ eV; Au, $E_m = 1{\cdot}12$ eV; Fe, $E_m = 0{\cdot}87$ eV. Inserting (22) into (21) we have a condition which, for any given T (this value being fixed by the desired segregation coefficient (19)), specifies the duration of the heat treatment. The above treatment is still oversimplified, because getter sites and metal impurities are supposed to be uniformly distributed inside the slice and the probability of visiting an already visited site has not been taken into account. The latter difficulty does not involve particular care, because the number of different sites visited in long walks is a constant fraction (about 66% for simple cubic lattice) of the total number of visited sites; the former difficulty, on the contrary, may be the decisive factor in establishing gettering conditions. For instance, removing heavy metals from active zones by segregation on the back of the slice may require higher temperature or longer time than segregation in the contacts or in the scribe lines. In the second case, heat treatment at 800°C for 10^3 s is usually sufficient. If, however, heavy metal atoms are present in precipitates, heat treatment at moderate temperature may be insufficient. Accordingly, a preliminary treatment at high temperature, say 1100°C, may be of help in dissolving metal precipitates (Baldi *et al.* 1979).

Remembering that gettering is useful only if gettered impurities are retained far from the active regions, we can summarize the previous considerations in the following operative criteria:

> getter sites must be formed out of active zones, for instance in the contacts or on the back;
> their concentration must be as high as possible, and their total number must be much greater than the total number of metal impurities;
> a higher temperature treatment must be performed if impurities are supposed to be in a precipitate form; and
> a final annealing at moderate temperature must be carried out to allow preferential segregation in getter sites.

If this procedure is directly superimposed on any standard device process before the metallization step, it represents the opposite approach to EG, where a sink of impurities is created on the back of the slice before any other process step.

Getter sites may differ greatly in chemical and physical nature. For instance, the following structures are, or at least are said to be, getter sites: poly-silicon, phosphorus–vacancy pairs, dislocations by phosphorus implantation, silicon–oxygen complexes.

For instance, Tseng *et al.* (1978) showed that after a segregation anneal, the gold profile "copies" the phosphorus profile, except in a dislocation-rich zone where gold is further accumulated. This example shows that both phosphorus and dislocations are effective getter sites. The gettering mechanism can vary widely from one structure to another, and no general features can be given.'

7.4. *Gettering and device process architecture*

Device processing is characterized by a relevant number of process steps: geometry definitions, layer depositions [dielectrics (Si_3N_4 and SiO_2), metals (aluminium), semiconductors (poly-silicon), polymers (resist)], etching, ion implantations, oxidations (dry or steam), predepositions, diffusion and anneals (inert or reducing atmospheres). The last four processes are thermal ones, the temperature and duration of which may be largely variable; for instance, a p- or n-well diffusion in complementary MOS involves temperatures around 1200°C for several hours in an inert atmosphere, while the Al:Si alloy process takes place at 450°C for about 30 min in a hydrogen atmosphere. The total number of fabrication steps is between 50 and 100, a half of which involve heat treatments.

Let us restrict our analysis to MOS processes, for which gettering techniques have been mainly developed. An MOS process can be thought of as chronologically organized in 4 segments, devoted to form:

(1) Wells	at	$T \simeq 1050$–1200°C
(2) Insulation and fields	at	$T \simeq 900$–1000°C
(3) Source and drain	at	$T \simeq 900$°C
(4) Metallization and protections	at	$T \simeq 450$°C

Segment 1 can be absent in n-channel MOS processes. Heat treatments of lower index segments are much heavier than those of higher index segments, so that the dopant profile resulting after lower index segment remains unchanged after subsequent heat treatments.

In this context, the three gettering techniques hold different positions: EG acts at level 0, IG starts at level 0 and operates up to level 4, while gettering by segregation acts between levels 3 and 4.

Acknowledgments

This work was read by several colleagues and friends. Though these colleagues do not necessarily share all our opinions, it is a pleasure to thank them: A. Armigliato and S. Solmi (Istituto LAMEL-CNR, Bologna), S. M. Hu (IBM General Technology Division, East Fishkill, NY), B. Pajot (Groupe de Physique des Solides, Université de Paris VII), S. Prussin (TRW, Redondo Beach, CA), and L. Reggiani (Department of Physics, University of Modena).

To remain within the size of a review paper, some topics—quantum-mechanical description of silicon phases, growth techniques, band-gap engineering, high-density limit (precipitates, clusters), silicon–metal interfaces, generation–recombination phenomena—have been omitted. This choice was dictated by our emphasis, mainly posed upon organicity, rather than on completeness, of presentation. However, since we hope to make up for this omission in the near future, we would greatly appreciate any comment on, or any updating of, the results presented here, as well as any suggestions of topics not considered here but which could be useful in a book on Physical Chemistry of, in and on Silicon.

We also express our acknowledgment to G. Butti for accurate typing.

References

ALLEN, W. G., and ANAND, K. V., 1971, *Solid St. Electron.*, **14,** 397.

ANTONIADIS, D. A., and DUTTON, R. W., 1979, *IEEE J. Solid St. Circuits*, **14,** 4122.

ANTONIADIS, D. A., GONZALES, A. G., and DUTTON, R. W., 1978, *J. Electrochem. Soc.*, **125,** 813.

BALDERESCHI, A., and HOPFIELD, J. J., 1972, *Phys. Rev. Lett.*, **28,** 171.

BALDI, L., CEROFOLINI, G. F., FERLA, G., and FRIGERIO, G., 1978 a, *Phys. Stat. Sol. a*, **48,** 523.

BALDI, L., CEROFOLINI, G. F., and FERLA, G., 1978 b, *154th Meeting of the Electrochemical Society*, Abstract 209.

BALDI, L., CEROFOLINI, G. F., and FERLA, G., 1979, *Surface Technol.*, **8,** 161.

BALDI, L., CEROFOLINI, G. F., and FERLA, G., 1980, *J. Electrochem. Soc.*, **127,** 125.

BARON, R., BAUKUS, J. P., ALLEN, S. D., MCGILL, T. C., KIMURA, H., WINSTON, H. V., and MARSH, O. J., 1979, *Appl. Phys. Lett.*, **34,** 257.

BARON, R., YOUNG, M. H., NEELAND, J. K., and MARSH, O. J., 1977, *Appl. Phys. Lett.*, **30,** 594.

BERGLUND, C. N., 1966, *IEEE Electron Dev.*, **13,** 701.

BOURRET, A., 1985, *Proceedings of the 13th International Conference on Defects in Semiconductors* (Warrendale, PA: The Metallurgical Society), p. 129.

BRONNER, G. B., and PLUMMER, J., 1984, *166th Meeting of the Electrochemical Society*, Abstract 483.

BUSTA, H. H., and WAGGENER, H. A., 1977 a, *J. appl. Phys.*, **48,** 4385.

BUSTA, H. H., and WAGGENER, H. A., 1977 b, *J. Electrochem. Soc.*, **124,** 1424.

CAMPISANO, S. U., JACOBSON, D. C., POATE, J. M., CULLIS, A. G., and CHEW, N. G., 1985, *Appl. Phys. Lett.*, **46,** 846.

CAPLAN, P. J., POINDEXTER, E. H., DEAL, B. E., and RAZOUK, R. R., 1979, *J. appl. Phys.*, **50,** 5847.

CAPPELLETTI, P., CEROFOLINI, G. F., and PIGNATEL, G. U., 1982 a, *J. appl. Phys.*, **53,** 6457.

CAPPELLETTI, P., CEROFOLINI, G. F., and PIGNATEL, G. U., 1982 b, *Phil. Mag.* A, **46,** 863.

CAPPELLETTI, P., CEROFOLINI, G. F., and POLIGNANO, M. L., 1985, *J. appl. Phys.*, **57,** 1406.

CAR, R., KELLY, P. J., OSHIYAMA, A., and PANTELIDES, S. T., 1984, *Phys. Rev. Lett.*, **52,** 1854.

CAZCARRA, V., and ZUNINO, P., 1980, *J. appl. Phys.*, **51,** 4206.

CEROFOLINI, G. F., 1983, *Phil. Mag.* B, **47,** 393.

CEROFOLINI, G. F., and FERLA, G., 1979, *156th Meeting of the Electrochemical Society*, Abstract 492.

CEROFOLINI, G. F., FERLA, G., and SPADINI, G., 1980, *Thin Solid Films*, **68,** 315.

CEROFOLINI, G. F., and FERLA, G., 1981, *Semiconductor Silicon 1981*, edited by H. R. Huff, R. J. Kriegler and Y. Takeishi (Pennington, NJ: The Electrochemical Society), p. 724.

CEROFOLINI, G. F., FERLA, G., PIGNATEL, G. U., RIVA, F., and OTTAVIANI, G., 1983 a, *Thin Solid Films*, **101,** 263.

CEROFOLINI, G. F., FERLA, G., PIGNATEL, G. U., and RIVA, F., 1983 b, *Thin Solid Films*, **101,** 275.

CEROFOLINI, G. F., FERLA, G., PIGNATEL, G. U., RIVA, F., NAVA, F., and OTTAVIANI, G., 1983 c, *Thin Solid Films*, **109,** 137.

CEROFOLINI, G. F., and POLIGNANO, M. L., 1984, *The Physics of VLSI*, edited by J. C. Knights (New York, NY: American Institute of Physics), p. 225.

CEROFOLINI, G. F., MEDA, L., QUEIROLO, G., ARMIGLIATO, A., SOLMI, S., NAVA, F., and OTTAVIANI, G., 1984, *J. appl. Phys.*, **56,** 2981.

CEROFOLINI, G. F., MANINI, P., MEDA, L., PIGNATEL, G. U., QUEIROLO, G., GARULLI, A., LANDI, E., SOLMI, S., NAVA, F., OTTAVIANI, G., and GALLORINI, M., 1985 a, *Thin Solid Films*, **129,** 111.

CEROFOLINI, G. F., PIGNATEL, G. U., MAZZEGA, E., and OTTAVIANI, G., 1985 b, *J. appl. Phys.*, **58,** 2204.

CEROFOLINI, G. F., MEDA, L., and OTTAVIANI, G., 1987, *Nucl. Instrum. Meth. B*, **19/20,** 488.

CEROFOLINI, G. F., and BEZ, R., 1987, *J. appl. Phys.*, **61,** 1435.

CHOU, M. Y., LOUIE, S. G., and COHEN, M. L., 1985, *Proceedings of the 17th International Conference on Physics of Semiconductors*, p. 43.

CLAEYS, C., BENDER, H., DECLERCK, G., VAN LANDUYT, J., VAN OVERSTRAETEN, R., and AMELINCKX, S., 1984, *Aggregation Phenomena of Point Defects in Silicon*, edited by E. Sirtl and J. Gorissen (Pennington, NJ: The Electrochemical Society), p. 74.

COTTON, F. A., and WILKINSON, G., 1980, *Advanced Inorganic Chemistry* (New York, NY: John Wiley & Sons).

CSEPREGI, L., KENNEDY, E. F., LAU, S. S., MAYER, J. W., and SIGMON, T, W., 1976, *J. appl. Phys.*, **29,** 645.

CSEPREGI, L., KENNEDY, E. F., GALLAGHER, T. J., MAYER, J. W., and SIGMON, T. W., 1977, *J. appl. Phys.*, **48,** 4234.
DAS, G., 1983, *Materials Research Society Symposium Proceedings*, Volume 14, p. 87.
DEAL, B. E., 1974, *J. Electrochem. Soc.*, **121,** 198C.
DEAL, B. E., 1980, *IEEE Trans. Electron Dev.*, **27,** 606.
DEAL, B. E., and GROVE, A. S., 1965, *J. appl. Phys.*, **36,** 3770.
DESSEAUX-THIBAULT, J., BOURRET, A., and PEUISSON, J. M., 1983, *Institute of Physics Conference Series*, Volume 67, p. 71.
DONOVAN, E. P., SPAEPEN, F., TURNBULL, D., POATE, J. M., and JACOBSON, D. C., 1983, *Appl. Phys. Lett.*, **42,** 698.
DONOVAN, E. P., SPAEPEN, F., TURNBULL, D., POATE, J. M., and JACOBSON, D. C., 1985, *J. appl. Phys.*, **57,** 1795.
EREMENKO, V. G., and NIKITENKO, V. I., 1972, *Phys. Stat. Sol. a*, **14,** 317.
FAHEY, P. M., 1985, Thesis, Stanford University, Stanford, CA.
FAHEY, P. M., BARBUSCIA, G., MOSLEHI, M., and DUTTON, R. W., 1985, *Appl. Phys. Lett.*, **46,** 784.
FAHEY, P. M., DUTTON, R. W., and MOSLEHI, M., 1983, *Appl. Phys. Lett.*, **43,** 683.
FAIR, R. B., 1977, *Semiconductor Silicon 1977*, edited by H. R. Huff and E. Sirtl (Princeton, NJ: The Electrochemical Society), p. 968.
FAIR, R. B., 1981, *J. Electrochem. Soc.*, **128,** 1360.
FAN, J. C. C., and ANDERSEN, H., 1981, *J. appl. Phys.*, **52,** 4003.
FISCHER, D. W., and MITCHEL, W. C., 1984, *Appl. Phys. Lett.*, **45,** 167.
FISCHER, D. W., and MITCHEL, W. C., 1985, *Appl. Phys. Lett.*, **47,** 281.
FÖLL, H., and CARTER, C. B., 1979, *Phil. Mag.* A, **40,** 497.
FRANK, W., 1975, *Institute of Physics Conference Series*, Volume 23, p. 23.
FULLER, C. S., 1956, *Rec. Chem. Progr.*, **17,** 75.
GALE, R., FEIGL, F. J., MAGEE, C. W., and YOUNG, D. R., 1983, *J. appl. Phys.*, **54,** 6938.
GEDDO, M., MAGHINI, D., and STELLA, A., 1986, *Solid St. Commun.*, **58,** 483.
GOETZBERGER, A., and SHOCKLEY, W., 1960, *J. appl. Phys.*, **31,** 1821.
GOETZBERGER, A., KLAUSMANN, E., and SCHULZ, M. J., 1976, *CRC Critical Reviews in Solid State Sciences*, Volume 1.
GÖSELE, U., FRANK, W., and SEEGER, A., 1982, *Solid St. Commun.*, **45,** 31.
GÖSELE, U., and TAN, T. Y., 1982, *Appl. Phys. A*, **28,** 79.
HANSEN, W. L., PEARTON, S. J., and HALLER, E. E., 1984, *Appl. Phys. Lett.*, **44,** 606.
HELMREICH, D., and SIRTL, E., 1977, *Semiconductor Silicon 1977*, edited by H. R. Huff and E. Sirtl (Princeton, NJ: The Electrochemical Society), p. 626.
HELMS, C. R., STRAUSSER, Y. E., and SPICER, W. E., 1978, *Appl. Phys. Lett.*, **33,** 767.
HELMS, C. R., JOHNSON, N. M., SCHWARZ, S. A., and SPICER, W. E., 1979, *J. appl. Phys.*, **50,** 1067.
HERRMANN, H., HERZER, H., and SIRTL, E., 1975, *Festkörperprobleme*, **15,** 279.
HU, S. M., 1977, *J. Vacuum Sci. Technol.*, **14,** 17.
HU, S. M., 1981, *J. appl. Phys.*, **52,** 3974.
HU, S. M., 1983, *Appl. Phys. Lett.*, **42,** 872.
HU, S. M., 1984, *J. appl. Phys.*, **55,** 4095.
HU, S. M., 1985, *VLSI Science and Technology 1985*, edited by W. M. Bullis and S. Broydo (Pennington, NJ: The Electrochemical Society), p. 465.
HU, S. M., 1986, *Appl. Phys. Lett.*, **48,** 115.
JAMES, H. M., and LARK-HOROVITZ, K., 1951, *Z. Phys. Chem., Leipzig*, **198,** 107.
JOHANNESEN, J. S., SPICER, W. E., and STRAUSSER, Y. E., 1976, *J. appl. Phys.*, **47,** 3028.
JOHNSON, N. M., 1985, *Phys. Rev.* B, **31,** 5525.
JONES, C. E., SCHAFER, D., SCOTT, W., and HAGER, R. J., 1981, *J. appl. Phys.*, **52,** 5148.
KAISER, W., FRISCH, H. L., and REISS, H., 1958, *Phys. Rev.*, **112,** 1546.
KANAMORI, A., and KANAMORI, M., 1979, *J. appl. Phys.*, **50,** 8095.
KITTEL, C., 1976, *Introduction to Solid State Physics* (New York, NY: John Wiley & Sons).
KITTEL, C., and MITCHELL, A. H., 1954, *Phys. Rev.*, **96,** 1488.
KOHN, W., 1957, *Solid St. Phys.*, **5,** 257.
KOLBESEN, B. O., and MÜLBAUER, A., 1982, *Solid St. Electron.*, **25,** 759.
KONDO, Y., 1981, *Semiconductor Silicon 1977*, edited by H. R. Huff, R. J. Kriegler and Y. Takeishi (Pennington, NJ: The Electrochemical Society), p. 220.

LANNOO, M., and BOURGOIN, J., 1981, *Point Defects in Semiconductors I* (Berlin: Springer-Verlag).
LARRABEE, R. D., THURBER, W. R., and BULLIS, W. M., 1980, *Semiconductor Measurement Technology* (Washington, DC: NBS), Special Publication 400-63.
LEUNG, M., and DREW, H. D., 1984, *Appl. Phys. Lett.*, **45,** 675.
LIPARI, N. O., THEWALT, M. L. W., ANDREONI, W., and BALDERESCHI, A., 1980, *Proceedings of the 15th International Conference on the Physics of Semiconductors*, p. 165.
LUTTINGER, J. M., and KOHN, W., 1955, *Phys. Rev.*, **97,** 969.
MASETTI, G., SOLMI, S., and SONCINI, G., 1973, *Solid St. Electron.*, **16,** 1419.
MASETTI, G., SOLMI, S., and SONCINI, G., 1976, *Solid St. Electron.*, **19,** 545.
MASTERS, B. J., and GOREY, E. F., 1978, *J. appl. Phys.*, **49,** 2717.
MATSUSHITA, Y., 1985, *Proceedings of the 17th International Conference on the Physics of Semiconductors*, p. 1525.
MAYER, H. J., MEHRER, H., and MAIER, K., 1977, *Institute of Physics Conference Series*, Volume 31, p. 186.
MAZZONE, A. M., 1985, *IEEE Trans. Computer Aided Design*, **4,** 110.
MEDA, L., CEROFOLINI, G. F., and OTTAVIANI, G., 1987, *Nucl. Instrum. Meth. B*, **19/20,** 454.
MEEK, R. L., and SEIDEL, T. E., 1975, *J. Phys. Chem. Solids*, **36,** 731.
MENDE, G., FINSTER, J., FLAMM, D., and SCHULZE, D., 1983, *Surface Sci.*, **128,** 169.
MILNES, A. G., 1973, *Deep Impurities in Semiconductors* (New York, NY: John Wiley & Sons).
MOORE, W. J., 1972, *Physical Chemistry* (Englewood Cliffs, NJ: Prentice Hall).
MORGAN, T. N., 1970, *Proceedings of the 10th International Conference on the Physics of Semiconductors*, p. 266.
MORITA, A., and NARA, H., 1966, *Proceedings of the 8th International Conference on the Physics of Semiconductors*, p. 234.
MURARKA, S. P., 1978, *J. appl. Phys.*, **48,** 5020.
MURARKA, S. P., SEIDEL, T. E., DALTON, J. V., DISHMAN, J. M., and READ, M. H., 1979, *156th Meeting of the Electrochemical Society*, Abstract 489.
NAG, B. R., 1972, *Theory of Electrical Transport in Semiconductors* (London: Pergamon Press).
NAGASAWA, K., MATSUSHITA, Y., and KISHINO, S., 1980, *Appl. Phys. Lett.*, **37,** 622.
NISHI, Y., 1966, *Jap. J. Appl. Phys.*, **5,** 333.
NISHI, Y., 1971, *Jap. J. Appl. Phys.*, **10,** 52.
OEHRLEIN, G. S., and CORBETT, J. W., 1983, *Materials Research Society Symposium Proceedings*, Volume 14, p. 107.
PANKOVE, J. I., CARLSON, D. E., BERKEYHEISER, J. E., and WANCE, R. O., 1983, *Phys. Rev. Lett.*, **51,** 2224.
PANKOVE, J. I., MAGEE, C. W., and WANCE, R. O., 1985 b, *Appl. Phys. Lett.*, **47,** 748.
PANKOVE, J. I., WANCE, R. O., and BERKEYHEISER, J. E., 1984, *Appl. Phys. Lett.*, **45,** 1100.
PANKOVE, J. I., ZANZUCCHI, P. J., MAGEE, C. W., and LUCOVSKY, G., 1985 a, *Appl. Phys. Lett.*, **46,** 421.
PANTELIDES, S. T., 1978, *Rev. Mod. Phys.*, **50,** 797.
PANTELIDES, S. T., 1984, *The Physics of VLSI*, edited by J. C. Knights (New York, NY: American Institute of Physics), p. 125.
PETROFF, P. M., ROZGONYI, G. A., and SHENG, T. T., 1975, *J. Electrochem. Soc.*, **122,** 565.
PLOUGOVEN, C., LEROY, B., ARHAN, J., and LECUILLER, A., 1978, *J. appl. Phys.*, **49,** 2711.
POINDEXTER, E. H., CAPLAN, P. J., DEAL, B. E., and RAZOUK, R. R., 1981, *J. appl. Phys.*, **52,** 879.
POLIGNANO, M. L., CEROFOLINI, G. F., BENDER, H., and CLAEYS, C., 1986, *ESPRIT '85*, edited by the COMMISSION OF THE EUROPEAN COMMUNITIES (Amsterdam: North-Holland), Part 1, p. 233.
PRUSSIN, S., 1985, *167th Meeting of the Electrochemical Society*, Abstract 255.
RAIDER, S. I., and BERMAN, A., 1978, *J. Electrochem. Soc.*, **125,** 629.
RAVA, P., GATOS, H. C., and LAGOWSKI, J., 1981, *Semiconductor Silicon 1977*, edited by H. R. Huff, R. J. Kriegler and Y. Takeishi (Pennington, NJ: The Electrochemical Society), p. 232.
RAY, I. L. F., and COCKAYNE, D. H. J., 1971, *Proc. R. Soc., Lond., Ser. A*, **235,** 543.
REGGIANI, L., 1980, *Proceedings of the 15th International Conference on the Physics of Semiconductors*, p. 317.
ROZGONYI, G. A., PETROFF, P. M., and READ, M. H., 1975, *J. Electrochem. Soc.*, **122,** 1725.
SAH, C. T., SUN, J. Y. C., and TZOU, J. J., 1983, *Appl. Phys. Lett.*, **43,** 204.
SAH, C. T., SUN, J. Y. C., and TZOU, J. J., 1984, *J. appl. Phys.*, **55,** 1525.

SCOTT, M. W., 1978, *Appl. Phys. Lett.*, **32,** 540.
SEARLE, C. W., OHMER, M. C., and HEMENGER, P. M., 1982, *Solid St. Commun.*, **44,** 1597.
SEARLE, C. W., HEMENGER, P. M., and OHMER, M. C., 1983, *Solid St. Commun.*, **48,** 995.
SECCO D'ARAGONA, F., 1972, *J. Electrochem. Soc.*, **119,** 948.
SEEGER, A., and FRANK, W., 1985, *Proceedings of the 13th International Conference on Defects in Semiconductors* (Warrendale, PA: The Metallurgical Society), p. 159.
SEEGER, A., and CHIK, K. P., 1968, *Phys. Stat. Sol. a*, **29,** 455.
SERVIDORI, M., ANGELUCCI, R., CEMBALI, F., NEGRINI, P., SOLMI, S., ZAUMSEIL, P., and WINTER, U., 1987, *J. appl. Phys.*, **61,** 1834.
SHIMURA, F., and CRAVEN, R. A., 1984, *The Physics of VLSI*, edited by J. C. Knights (New York, NY: American Institute of Physics), p. 205.
SHINOHARA, S., 1961, *Nuovo Cimento*, **22,** 18.
SOLOMON, P. M., 1984, *The Physics of VLSI*, edited by J. C. Knights (New York, NY: American Institute of Physics), p. 172.
STRACK, H., MAYER, K. R., and KOLBESEN, B. O., 1979, *Solid St. Electron.*, **22,** 135.
TAN, T. Y., GARDNER, E. E., and TICE, W. K., 1977, *Appl. Phys. Lett.*, **30,** 175.
TAN, T. Y., and GÖSELE, U., 1985, *Appl. Phys.* A, **37,** 1.
TAN, T. Y., FÖLL, H., and HU, S. M., 1981, *Phil. Mag.* A, **44,** 127.
TANIGUCHI, K., ANTONIADIS, D. A., and MATSUSHITA, Y., 1983, *Appl. Phys. Lett.*, **42,** 961.
TANIGUCHI, K., KUROSAWA, K., and KASHIWAGI, M., 1980, *J. Electrochem. Soc.*, **127,** 2243.
THOMPSON, D. A., GOLANSKI, A., HAUGER, K. H., STEFANOVIC, D. V., CARTER, G., and CHRESTOULIDES, C. E., 1980, *Rad. Eff.*, **52,** 69.
TSENG, W. F., KOJI, T., MAYER, J. W., and SEIDEL, T. E., 1978, *Appl. Phys. Lett.*, **33,** 442.
VAN VECHTEN, J., 1974, *Phys. Rev.* B, **10,** 1482.
VAN VECHTEN, J., 1985, *Proceedings of the 13th International Conference on Defects in Semiconductors* (Warrendale, PA: The Metallurgical Society), p. 293.
WATKINS, G. D., and CORBETT, J. W., 1961, *Phys. Rev.*, **121,** 1001.
WATKINS, G. D., 1975, *Institute of Physics Conference Series*, Volume 23, p. 1.
WATKINS, G. D., 1979, *Institute of Physics Conference Series*, Volume 46, p. 16.
WERTHEIM, G. K., 1959, *Phys. Rev.*, **115,** 568.
WOLF, H. F., 1969, *Silicon Semiconductor Data* (Oxford: Pergamon Press).
WU, Y., and FALICOV, L. M., 1984, *Phys. Rev.* B, **29,** 3671.
YAMAMOTO, K., KISHINO, S., MATSUSHITA, Y., and IZUKA, T., 1980, *Appl. Phys. Lett.*, **36,** 195.
YIN, M. T., 1985, *Proceedings of the 17th International Conference on the Physics of Semiconductors*, p. 927.
YIN, M. T., and COHEN, M. L., 1980, *Phys. Rev. Lett.*, **45,** 1004.
YIN, M. T., and COHEN, M. L., 1982, *Phys. Rev.* B, **26,** 5668.
ZULEHNER, W., and HUBER, D., 1982, *Crystals*, **8,** 1.